Searching for new light particles and X17 at PADME

Venelin Kozhuharov

Faculty of Physics, Sofia University and LNF-INFN

18th Workshop on Particle Correlations and Femtoscopy

May 18-22, 2026, Budapest, Hungary

Bulgarian National Roadmap for Research Infrastructures - object CERN

X17 anomalies

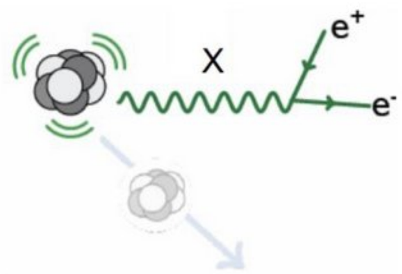

PRL 116 (2016

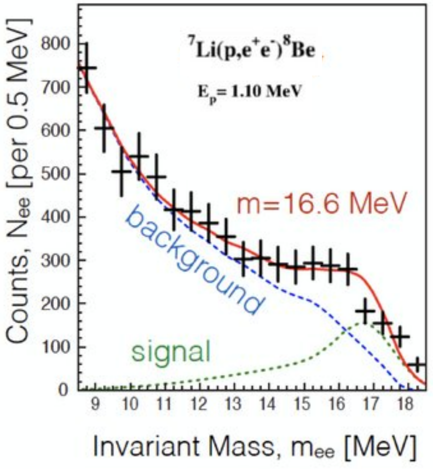

Phys. Rev. C 106, L061601 (**2022**)

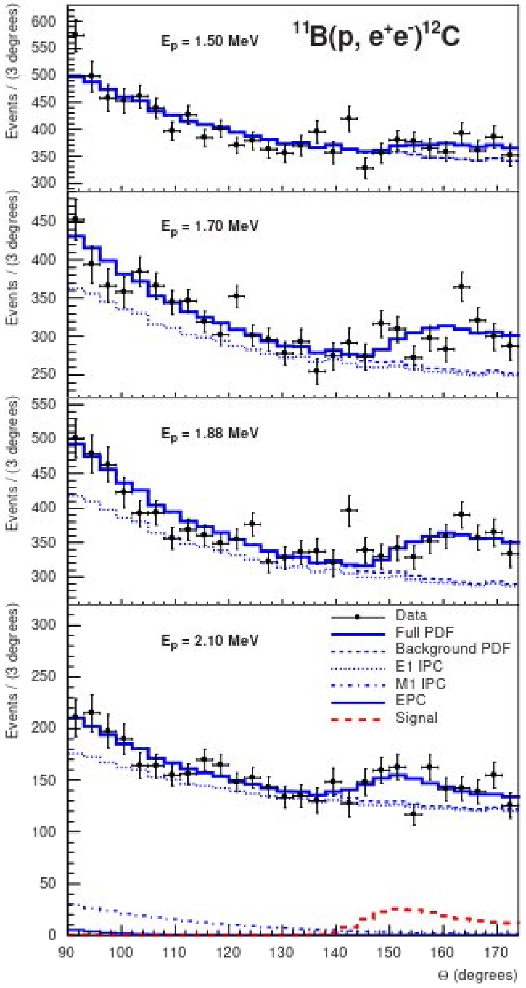

Phys.Rev.C 104, 044003 (**2021**)

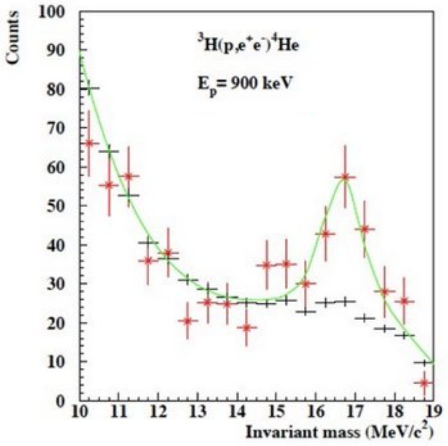

Similar observables in the **^{8}Be**, **^{4}He** and **^{12}C** experiments:

- 2 leptons in the final state
- Kinematics properties determined by the mass of the X17 particle (2 body decays)
- M_{X17} = 16.85 ± 0.04 MeV
  (Phys. Rev. D 108, 015009)

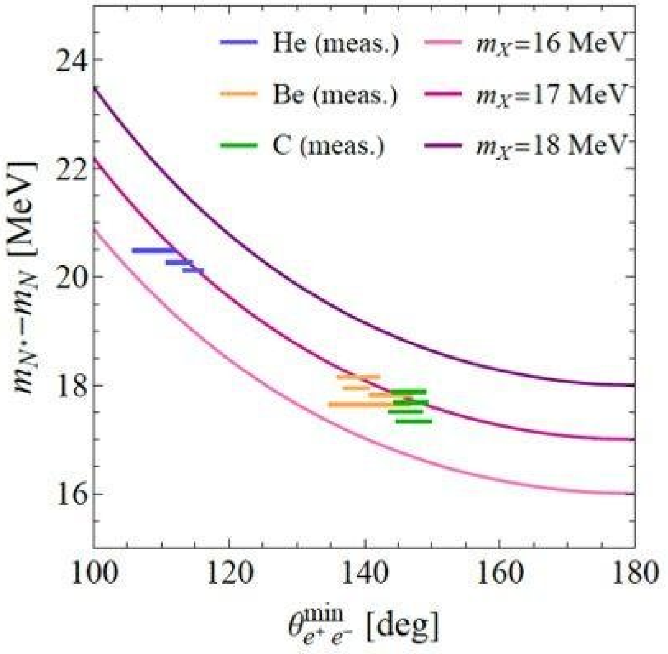

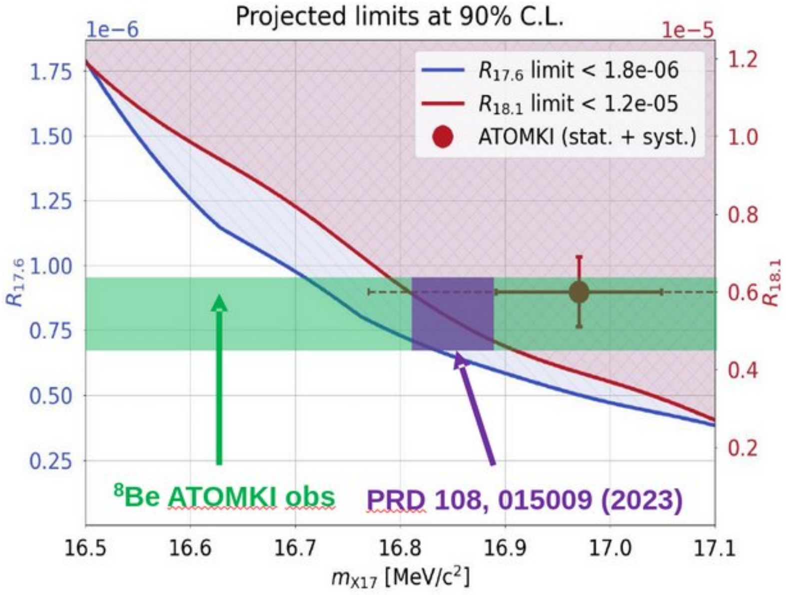

- **MEG2**: Measurement on ^{7}Li target to reproduce ^{8}Be ATOMKI result
- ULs on **BR(^{8}Be*→ ^{8}Be + e^{+}e^{-}, anomaly) / BR(^{8}Be* → ^{8}Be + ɣ)** for 17.6 MeV, 18.1 MeV transitions
- The MEG-II result remains compatible (*JHEP 04 (2025) 035*) with *PRD 108, 015009 (2023)*

New light particles in e$^+$ on target annihilation

Accelerated e$^+$ impinging on a thin target

- **Associate production: $e^+e^- \rightarrow \gamma + X$**
  - Measurement of the recoil photon in the calorimeter
  - Suppress all the background with at least 1 photon in the final state
  - Search for bumps in $M^2_{miss} = (P_{e+} + P_{e-} - P_{\gamma})^2$ distribution
- **Bremsstrahlung: $e^+ + Z \rightarrow e^+ + Z + X$**
- **Resonant production: $e^+e^- \rightarrow X$**
  - $M^2_{inv} = s \sim 2\, E_{beam}\, m_e$
  - No additional particle in the final state - without tagged primary positrons X should decay to provide a **visible signature**: $X \rightarrow e^+e^-$
  - Scan the excess of e^+e^- final states as function of $\mathbf{E_{beam}}$ (i.e. M_{inv} or $\sqrt{s}$)

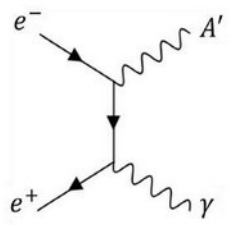

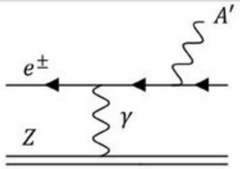

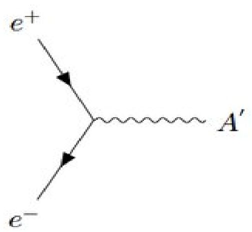

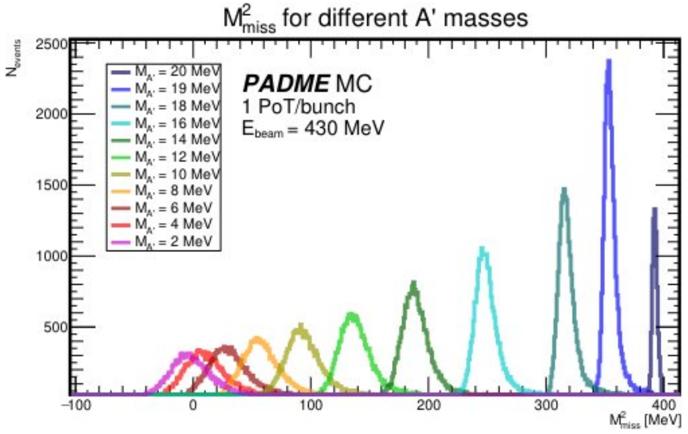

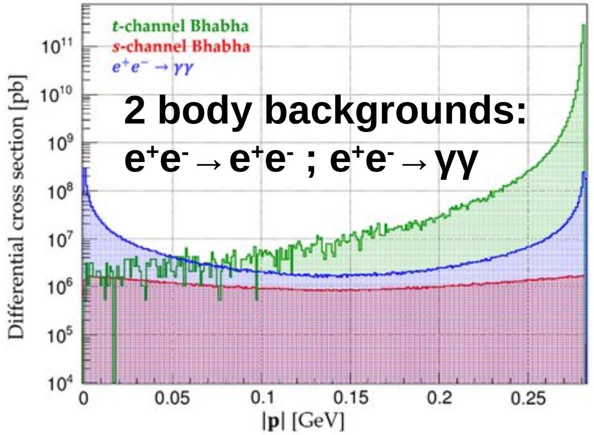

$$\mathcal{N}^{\text{Vect.}}_{X_{17}} \simeq 1.8 \cdot 10^{-7} \times \left(\frac{g_{ve}}{2 \cdot 10^{-4}}\right)^2 \left(\frac{1\ \text{MeV}}{\sigma_E}\right)$$

$$\mathcal{N}^{\text{ALP}}_{X_{17}} \simeq 5.8 \cdot 10^{-7} \times \left(\frac{g_{ae}}{\text{GeV}^{-1}}\right)^2 \left(\frac{1\ \text{MeV}}{\sigma_E}\right)$$

Darme et al. Phys. Rev. D 106, 115036

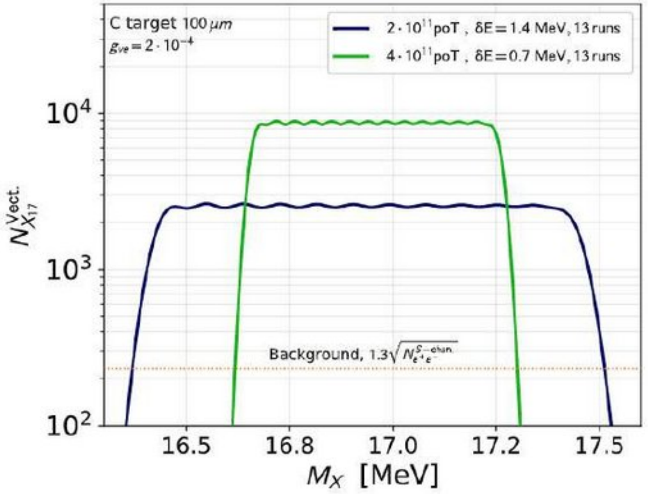

Measurement of e^+e^- final states at different $\sqrt{s}$

$$\frac{N(e^+e^-)}{N_{PoT}}$$

$$\frac{N(e^+e^- + \gamma\gamma)}{N_{PoT}}$$

$$\frac{N(e^+e^-)}{N(\gamma\gamma)}$$

Different strategies

Different systematics

PADME: Positron on target annihilation

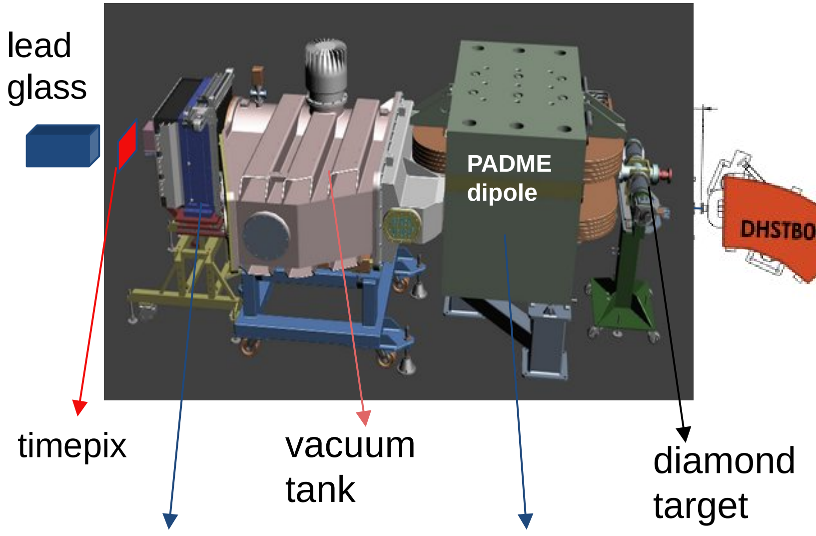

Combination of fixed target and collider techniques

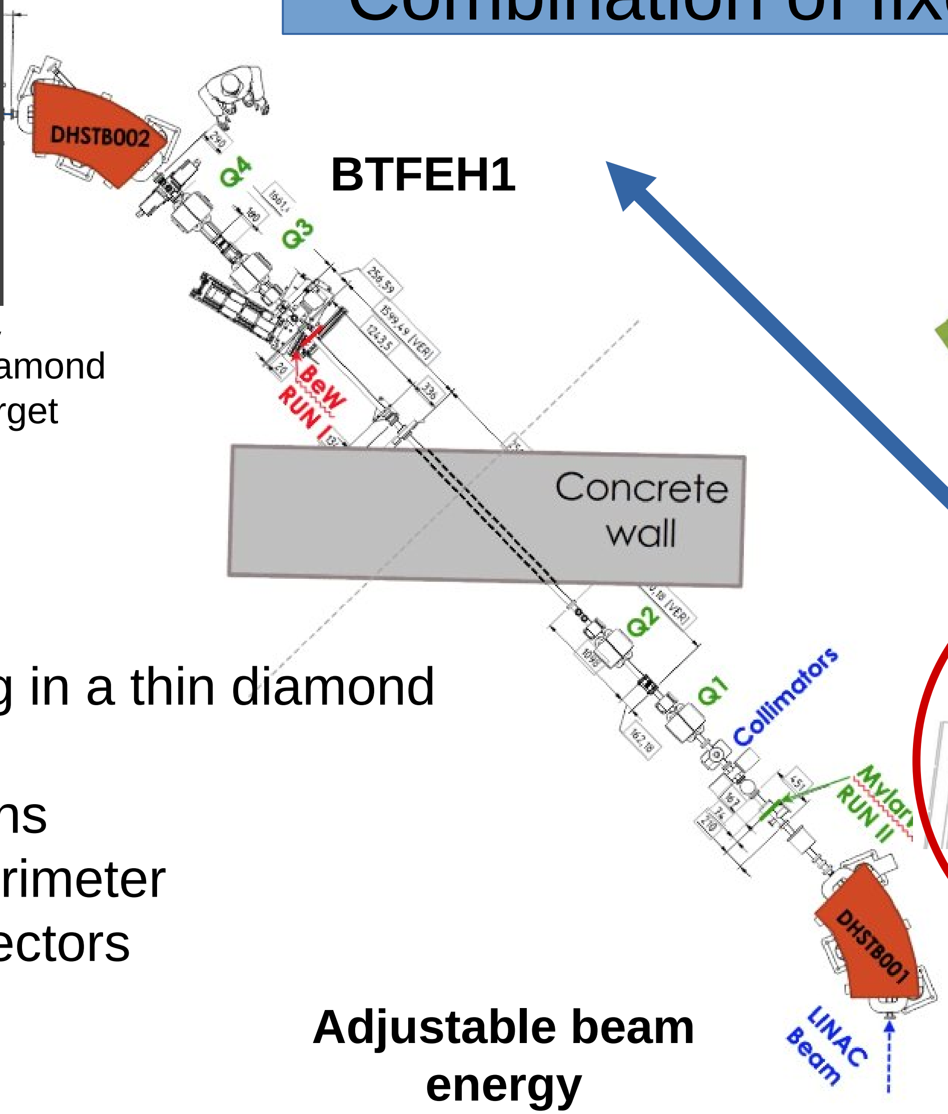

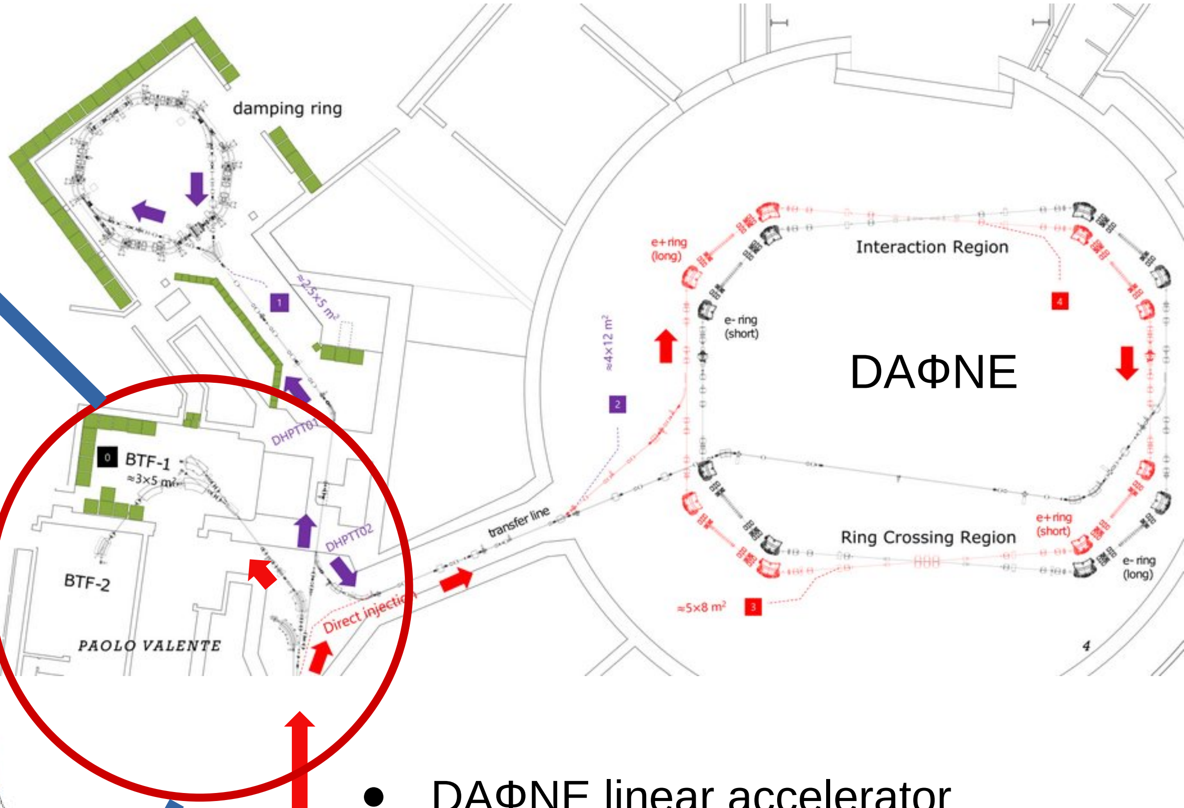

- Accelerated e⁺ interacting in a thin diamond active target
- Final states: e⁺, e⁻, photons
  - Electromagnetic calorimeter
  - Charged particle detectors
- Beam measurement
  - Timepix
  - Lead Glass

Adjustable beam energy
100 MeV - 500 MeV

- DAΦNE linear accelerator
  - 50 bunches/s (1 for monitoring)
  - e+/e-
  - Up to O(300ns) macro-bunches
- BTF beam spot: 1 mm
- Beam divergence: 1-1.5 mrad

PADME RUN III: Resonant X17 production

Running with no magnetic field in PADME dipole

$e^+e^- \rightarrow X17 \rightarrow e^+e^-$

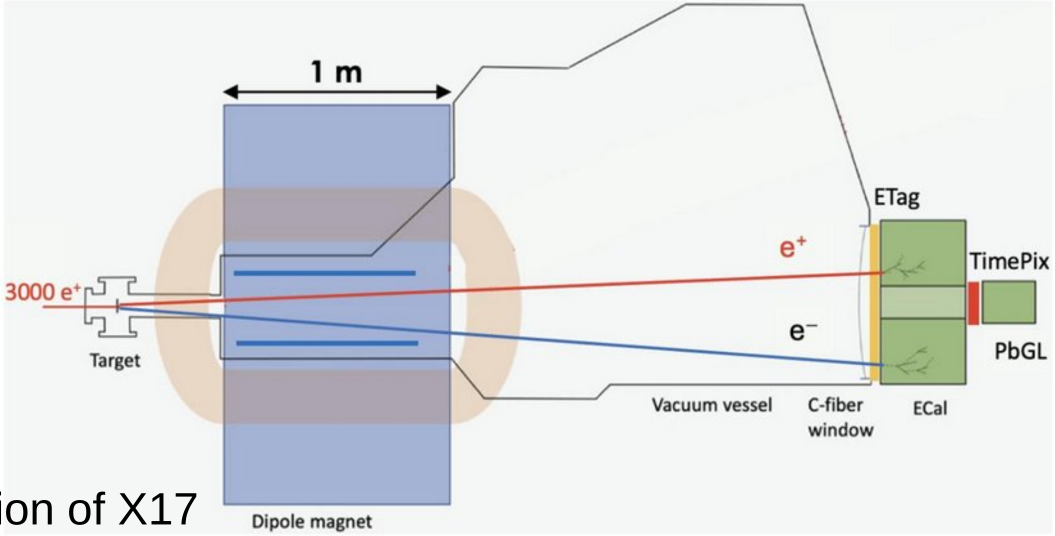

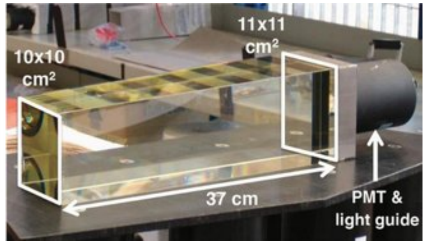

JHEP 2024, 2024(8), 121

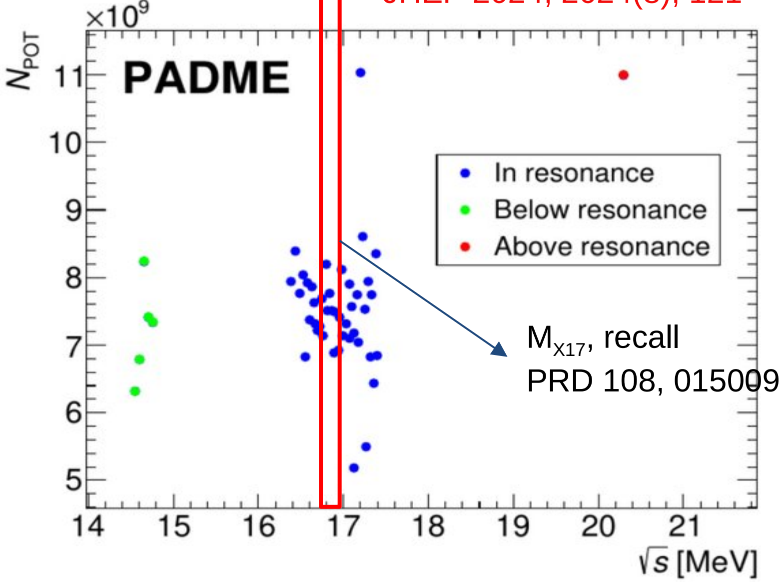

- On-shell production of X17
- Scan and search for a change in **$\sigma(e^+e^- \rightarrow e^+e^-)$ as function of $\sqrt{s}$**
- 47 points, 263 MeV < E_{beam} < 299 MeV
  - 16.4 MeV < M_{X17} < 17.5 MeV
  - Energy step: 0.7 MeV
  - Mass step: ~ 20 keV
- 5 points below resonance
  - 205 MeV < E_{beam} < 211 MeV
- 1 point with E_{beam} = 402 MeV
- Low (compared to RUN I & II) beam intensity: O(3000) e^+/bunch

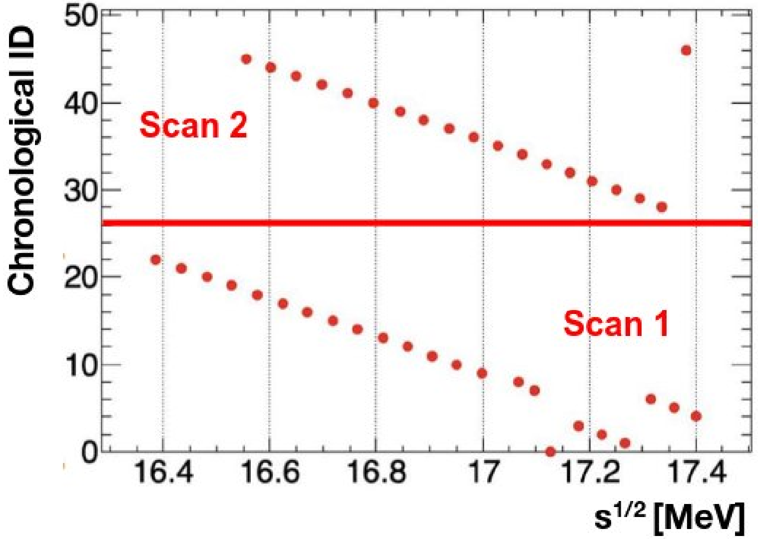

Probing X17 in resonant production

- PADME RUN III strategy: measure all two cluster events $\mathbf{N_2(s)}$ and normalize to number of positrons on target, i.e discriminate

$$N_2(s) = N_{PoT}(s) \times [\, B(s) + S(s; M_{X17}, g)\ \ \varepsilon_S(s)\,] \text{ vs } N_2(s) = N_{PoT}(s) \times B(s)$$

  - $\mathbf{N_{PoT}}$ - positrons on target
  - **B(s)** - background yield per PoT
  - $\mathbf{S(s,M_{X17},g)}$ - signal production as a function of mass and coupling
  - $\boldsymbol{\varepsilon_S(s)}$ - signal selection efficiency
  - **√s** - measured from E_{beam} run by run

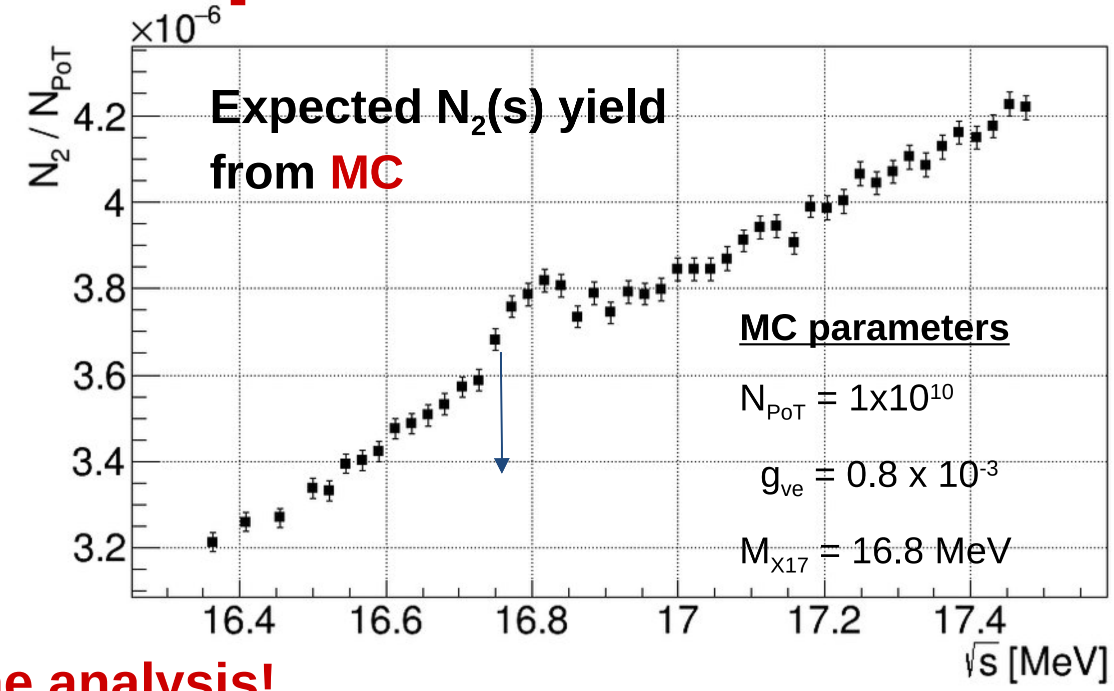

$N_2(s)$ is kept blind throughout the analysis!

MC with M_X = 16.8 MeV, g_v = 8×10^{-4}

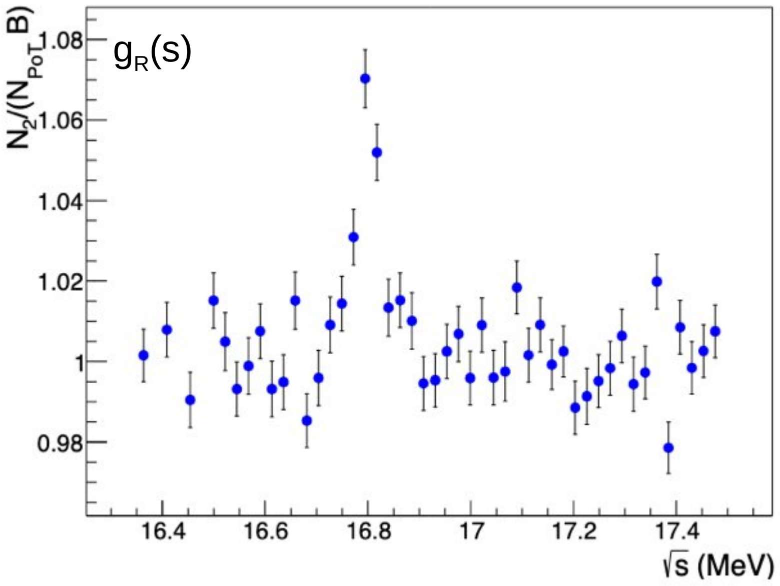

- Exploit possible systematics cancellations through ratios and ratio parametrizations
- Experimental observable

$$g_R(s) = N_2(s) \,/\, (\, N_{POT}(s)\ B(s)\,)$$

- In ideal world with all effects properly considered

$$g_R(s) = [\, 1 + S(s; M_X, g)\ \varepsilon_S(s) \,/\, B(s)\,]$$

  - In the absence of signal $g_R(s) \cong 1$
- Various effects may induce linear scale deviation in $g_R(s)$

Events selection

- Select any two-body final state in the ECal acceptance
- R_{max} away from ECal edges by more than 1 crystal
- Compute R_{min}, E_{min}, E_{max}
- Cluster pairs selection:
  - $E > E_{min} \times 0.4$
  - $\Delta t < 5$ ns
  - First cluster: within (R_{min} - D, R_{max}), D = 1.5 crystals
  - Second cluster with $R > R_{min}$ - D

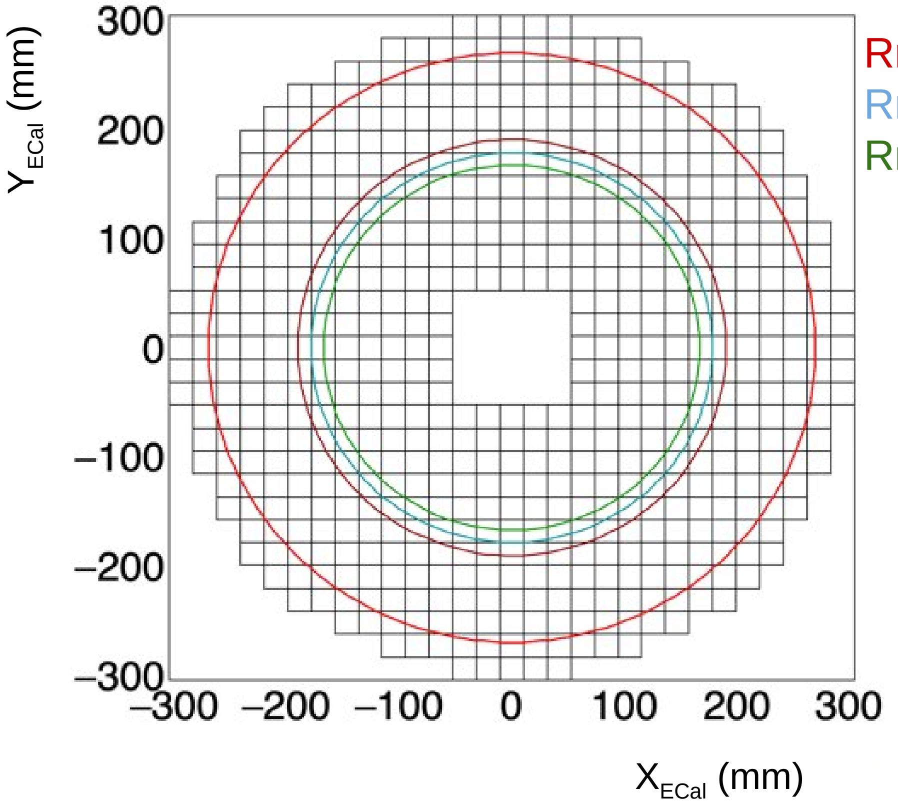

Selection region
Sideband region

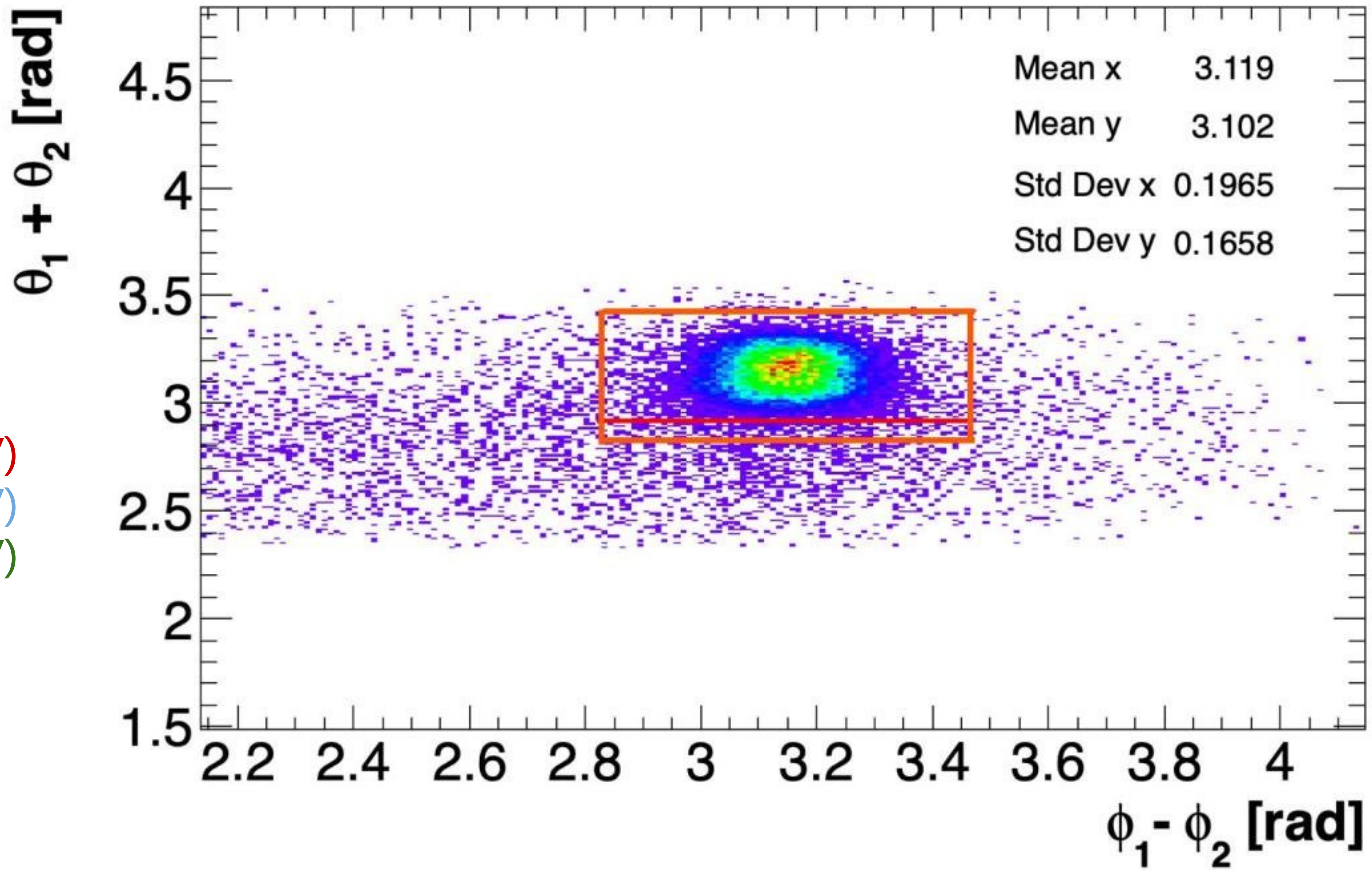

- Select back-to-back pairs in the center of mass frame
  - 2 body final state kinematics
  - Center of mass angles quasi-independent from lab energy
    - Up to m_e/E terms

Event selection: beam variation

JINST 19 (2024) 01, C01016

Timepix 3 array

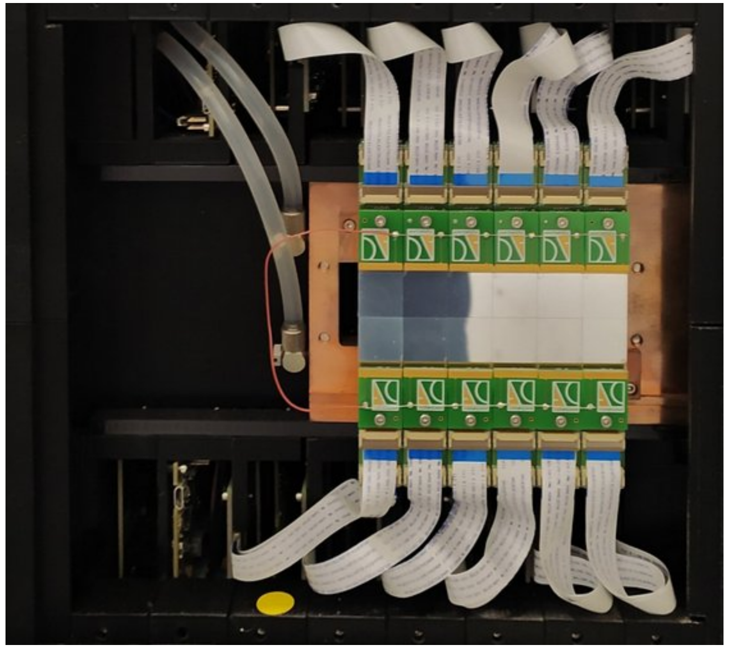

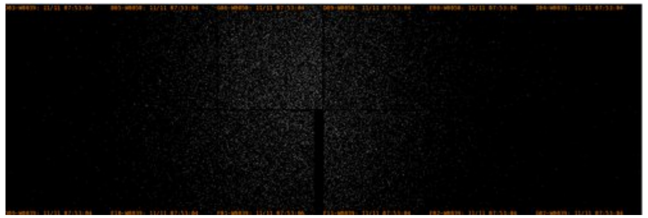

- Matrix of 2 x 6 Timepix3 detectors
  - each 256x256 pixels
- Operated in 2 modes:
  - image mode, integrating
  - streaming mode, feeding ToT and ToA for each fired pixel

COG at the ECal front face from 2 cluster events

Movement within 10 mm

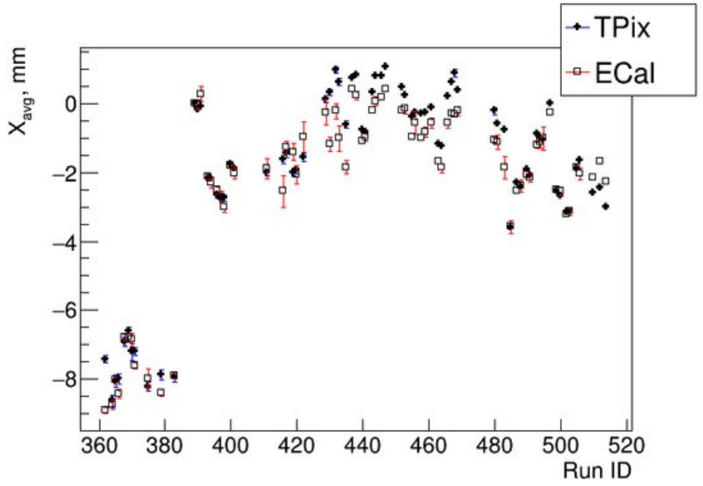

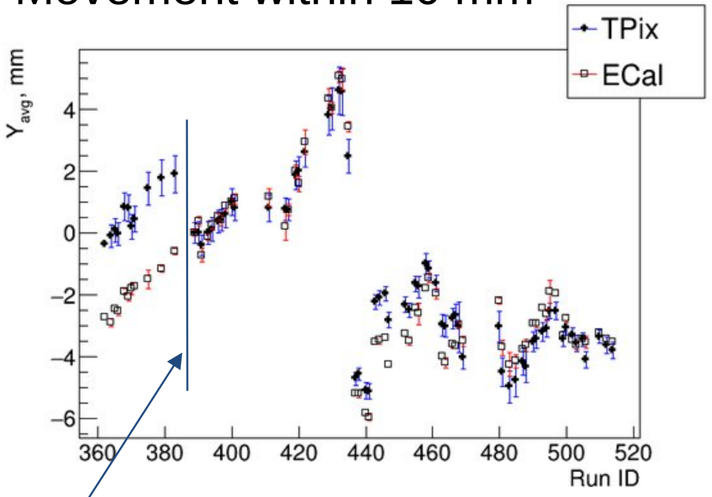

Timepix was moved by 1.8 mm

JHEP 08 (2024) 121

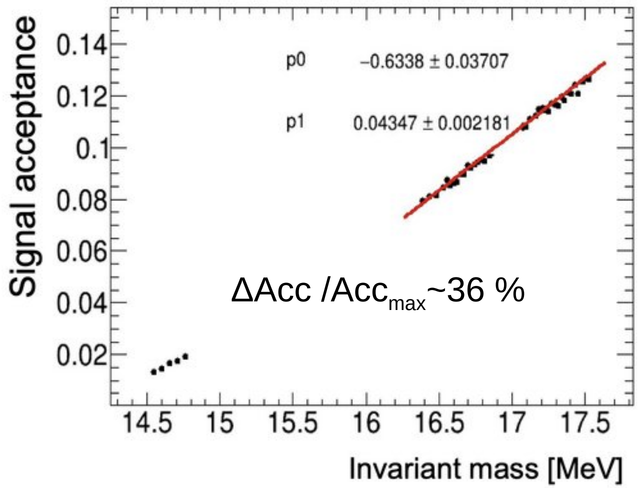

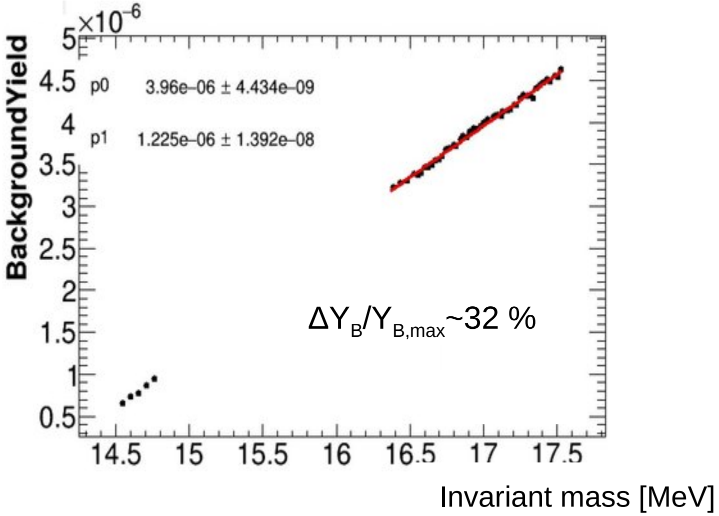

Events selection

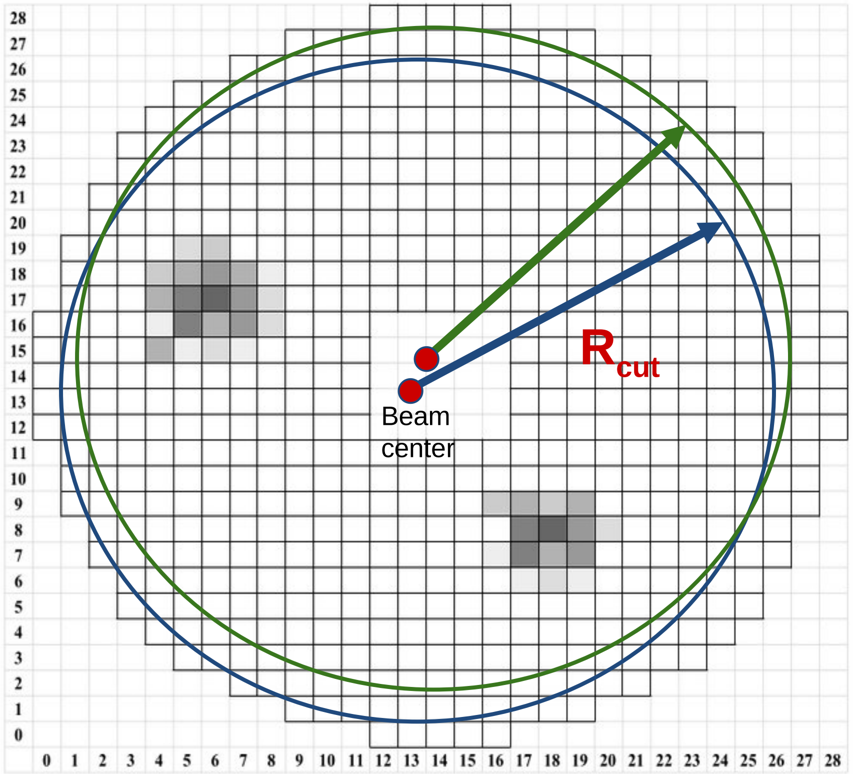

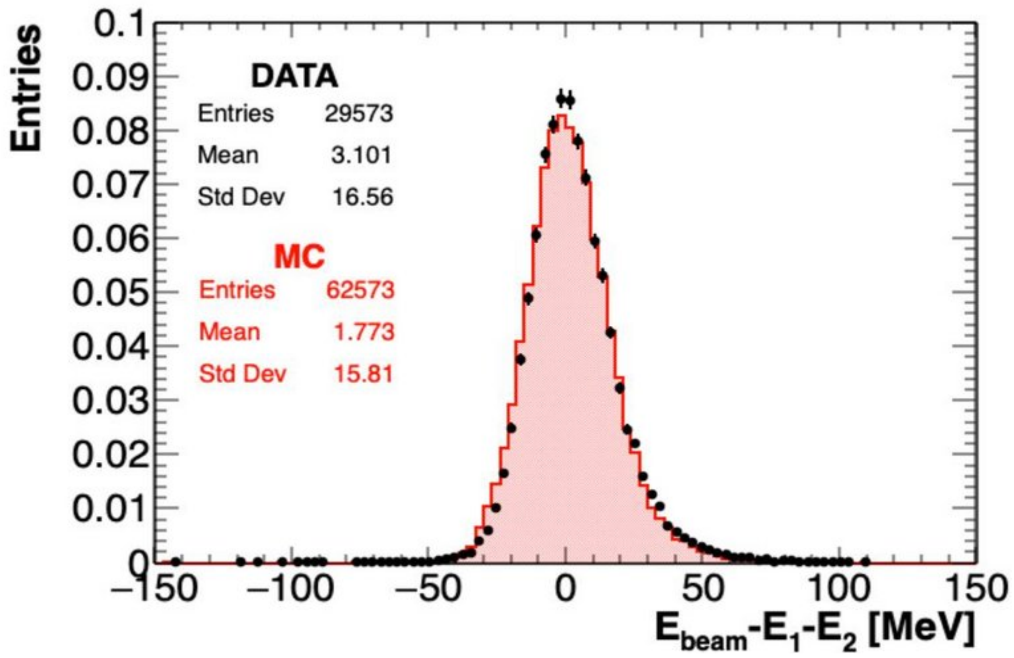

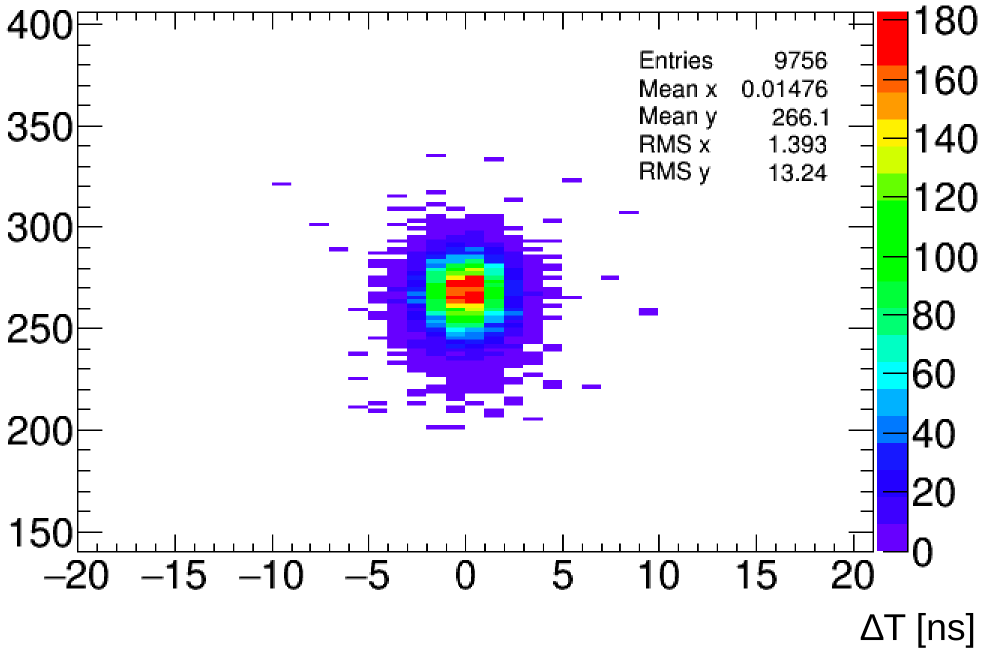

- Selection algorithm independent on the beam variation
  - Beam center determination run by run (with better than mm precision)
  - Marginal use of the cluster energy in the selection due to the proper choice of the selection variables
- N_2 counts around 30k / period
  - δN_2 ~ 0.6% to 0.7%
  - Selected events with 4 % background
    - bremsstrahlung in the target, uncertainty ~ 0.3%

Expected background per e^+: B

Determined with MC + data-driven checks

B($s^{1/2}$)

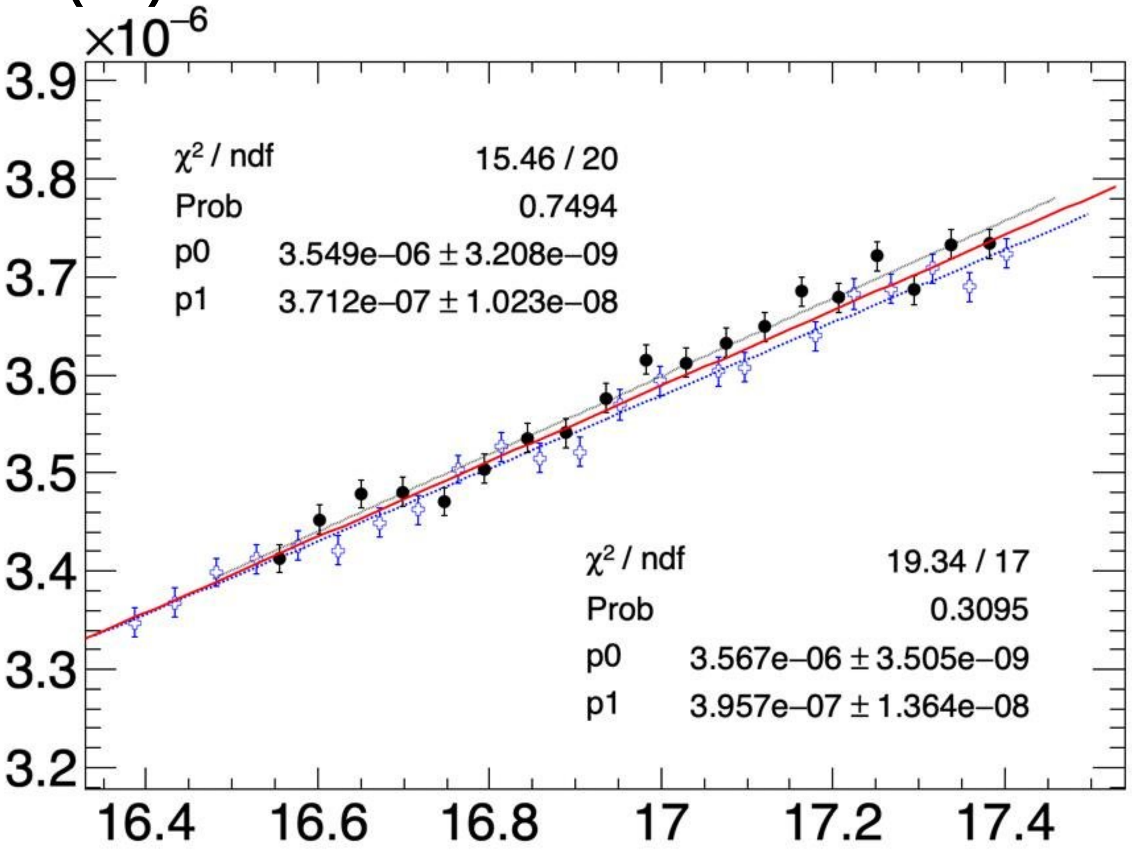

$s^{1/2}$ (MeV)

- B expectation is compared to below resonance points, improving the systematic uncertainty
- Fit of B($s^{1/2}$) with a straight line [*used only as a check*]; background curve slightly depending on the scan
- B($s^{1/2}$) per period used in the analysis

Uncorrelated uncertainty budget

Source	Uncertainty on B per period [%]
MC statistics	0.4
Data/MC (Tag&Probe)	0.2
Cut stability	0.2
Beam spot	0.1
Total	0.5

- Correlated (common) systematic errors on B enter in the scale K(s), e.g.: absolute cross section (rad. corr. at 3%), target thickness
- Total correlated uncertainty: 0.6%

Positron flux measurement

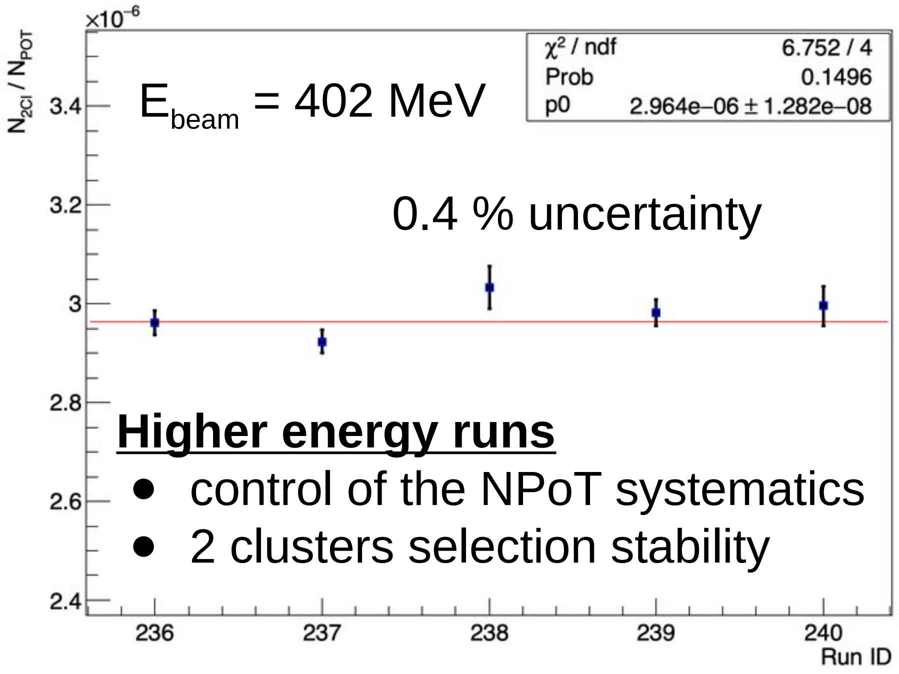

E_{beam} = 402 MeV

0.4 % uncertainty

<u>Higher energy runs</u>

- control of the NPoT systematics
- 2 clusters selection stability

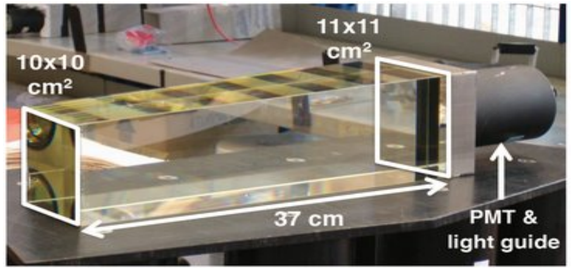

N_{PoT} determination from Q_{LG}

$$N_{POT} = Q_{LG} / Q_{1e+, 402\ MeV} \times 402 / E_{beam}\ [\mathrm{MeV}]$$

- Common systematics ~ 2%, JHEP 08 (2024) 121
- Energy scale from Timepix spot size: 0.3%

Leakage ⟵ **corrections** ⟶ Aging

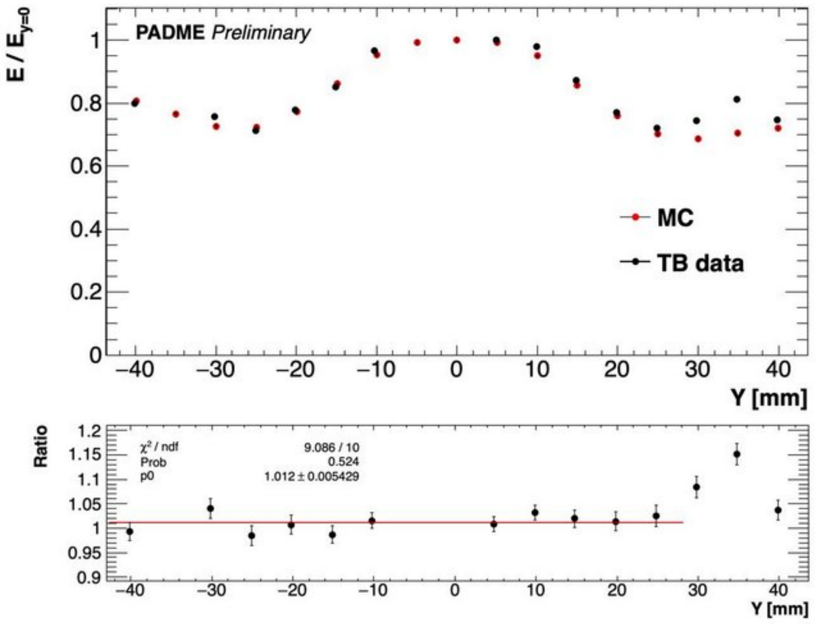

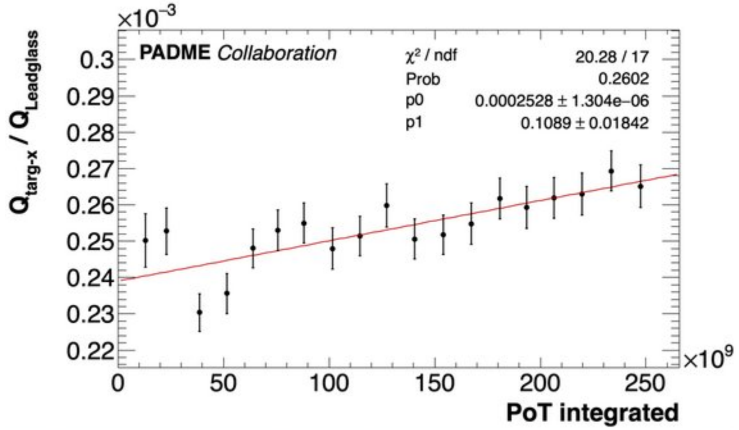

- PoT is primarily measured by an OPAL lead glass block downstream of the setup
- Additional detectors to control the PoT systematics
  - and to derive correction factors
- Several testing campaigns
  - A few positrons → clear 1e, 2e, etc. peak identification
  - O(2000) PoT - cross-calibration with the BTF FitPix

- Uncorrelated error: 0.45 % (energy scale + aging slope)
- Common error: 2.1 %

PADME RUN III sensitivity

Uncorrelated systematics

Source	Uncertainty [%]
N_2	0.6
N_{PoT}	0.35
B	0.55
Total on g_R	0.89

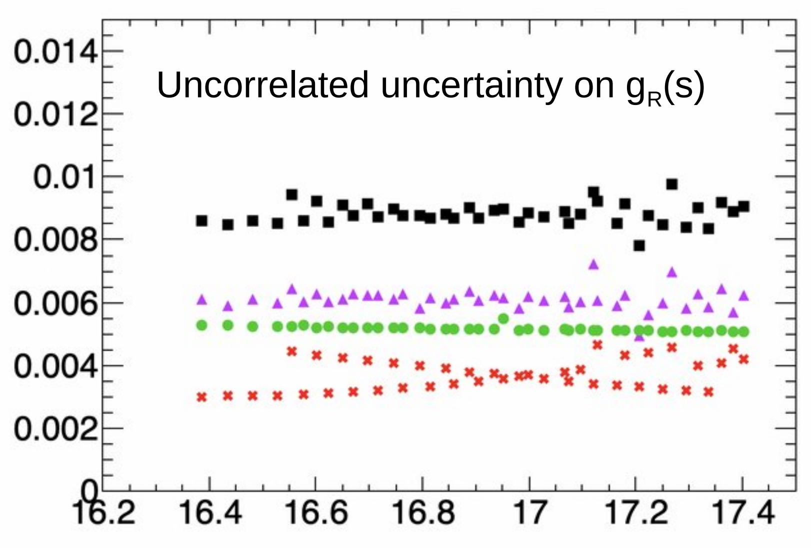

Following ATL-PHYS-PUB-2011-11 & CMS NOTE-2011/005

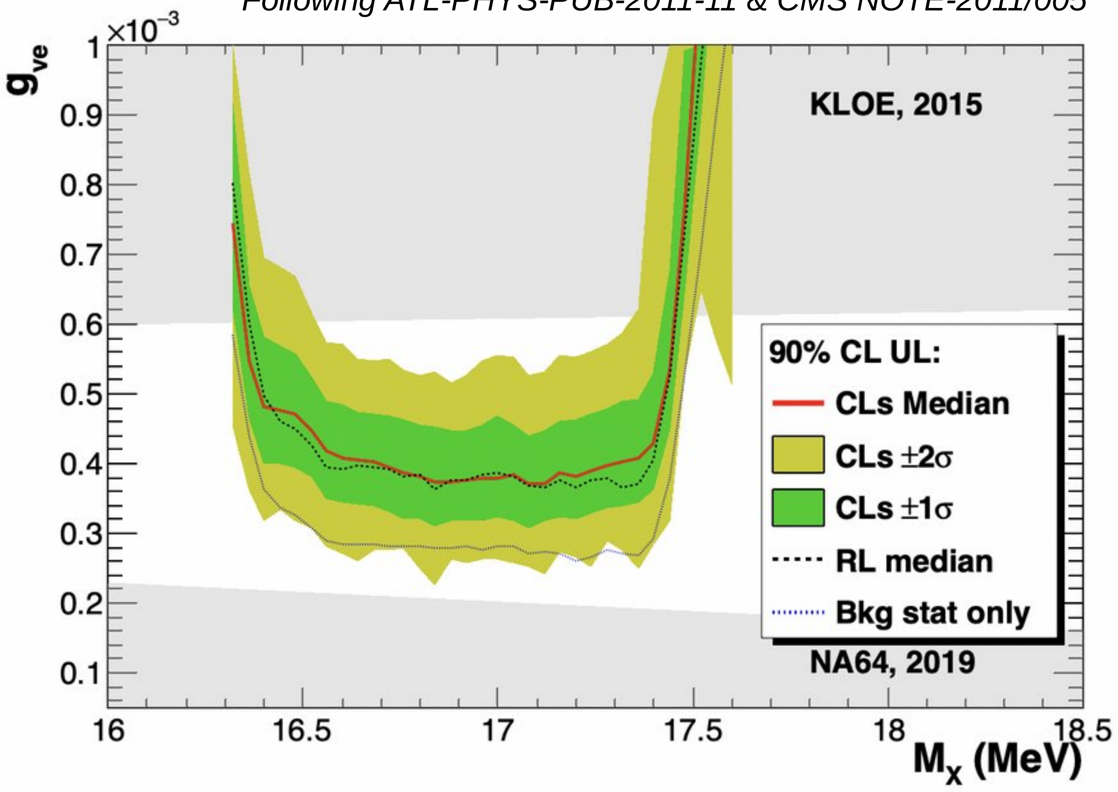

For details, JHEP 06 (2025) 040

- p_S and p_B are obtained using simulations, where the observables are always sampled, while the nuisance parameters stick to the B and S+B fits ("hat")
- Also shown for comparison only:
  - the median of the limits obtained using the Rolke-Lopez likelihood-ranking method
  - the purely statistical UL, $1.28\ N_2^{1/2}$

- Evaluate expected 90% CL UL in absence of signal
- Define $Q_{statistic}$ based on Likelihood ratio: $Q = L_{S+B}(g_v, M_X) / L_B$
- The likelihood includes terms for each nuisance parameter pdf
- For a given M_X, $CLs = p_S / (1 - p_B)$ is used to define the UL on g_{ve}
- Asimov test performed (asymptotic limit)

"Open the box" in two steps: data self-consistency and looking for X17

Data self-consistency ("blind unblinding")

JHEP 06 (2025) 040

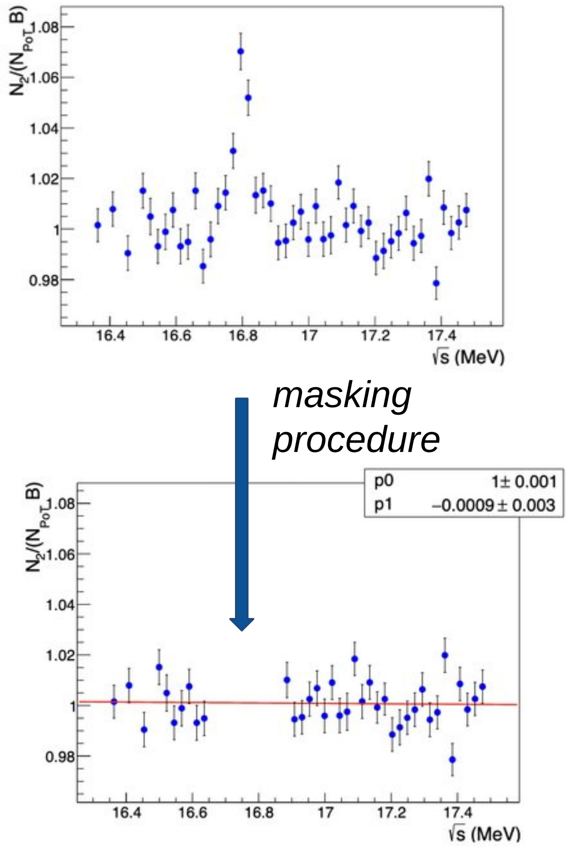

- Define a side-band in $g_R(s)$, excluding 10 consecutive in $s^{1/2}$ periods of the scan by maximizing the probability for a linear fit
- Define criteria to be respected by the remaining data points before proceeding to box opening:
  1. Threshold on the χ^2 fit in side-band is $P(\chi^2)$ = 20%,
     - Defined through 90 % acceptance probability (reject 10 % of the times)
  1. Check if the fit pulls with respect to the line fit follow Gaussian distribution
  2. Check if a straight-line fit of the pulls has no slope in $s^{1/2}$ (within 2 sigma)
  3. Check if the constant term and slope of the linear fit for K(s) are within two sigma of the expectations, i.e.: 1.0 ± 4% for the constant, ± 2% MeV^{-1} for the slope

A failure at any step of the procedure would forbid box opening and would lead to a step back to analysis

Applied to data:

1. **$P(\chi^2)$ = 74%**
2. **Pulls gaussian fit probability 60%**
3. **Slope of pulls consistent with zero**
4. **Constant term = 1.0116 (16), Slope = (-0.010 ± 0.005) MeV^{-1}**

PROCEED TO BOX OPENING

Ublinding the result

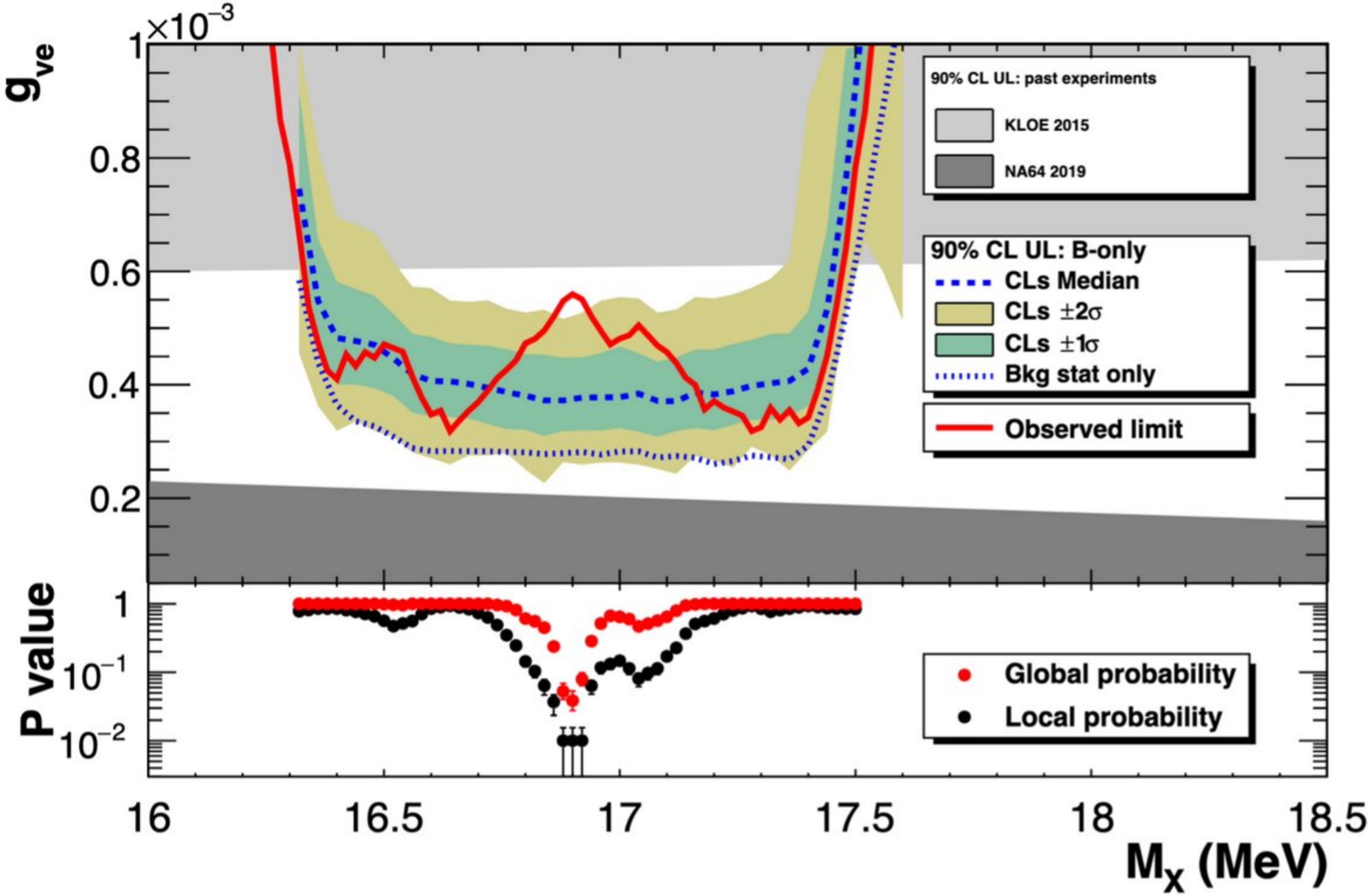

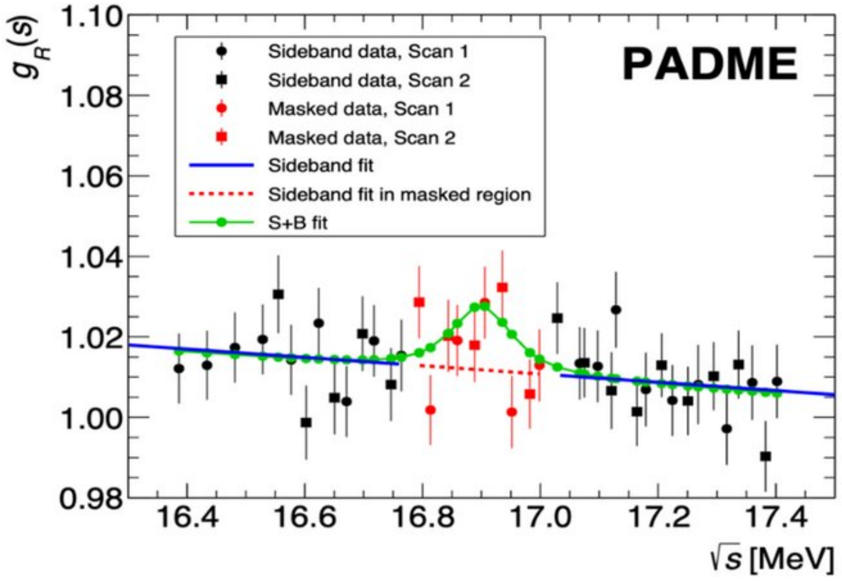

- At M_X = 16.90(2) MeV, g_{ve} = 5.6 x 10^{-4}, the global probability dip reaches 3.9 $_{-1.1}^{+1.5}$ %,
  - corresponding to (1.77 ± 0.15) one-sided (look-elsewhere calculated exactly from the toy pseudo-events)

- The observed limit is consistent with the expected within 1 sigma in most of the scan interval
  - Verification of the analysis robustness and uncertainty estimations
- Slight excess observed beyond the 2 σ local coverage

Ublinding the result

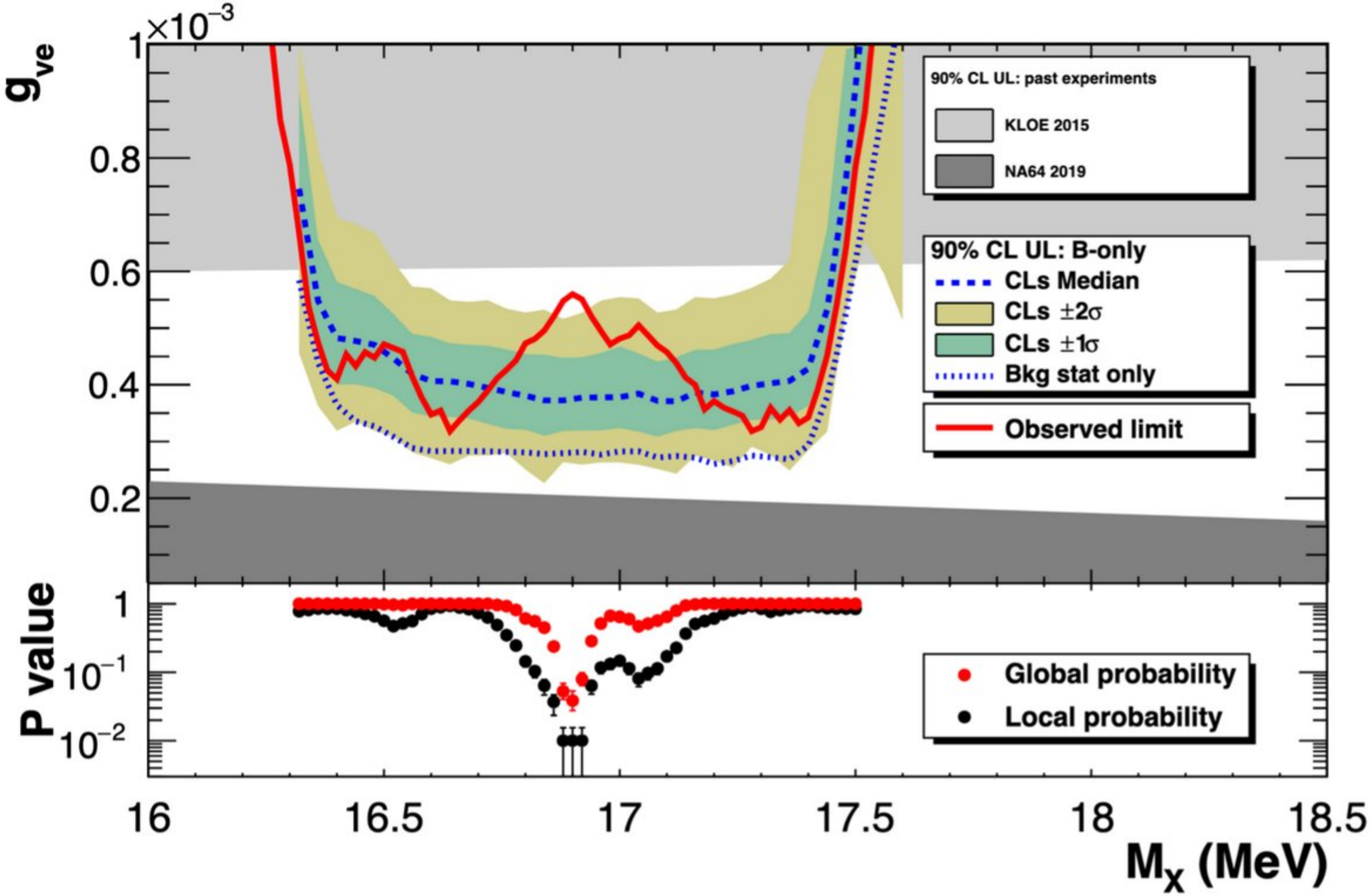

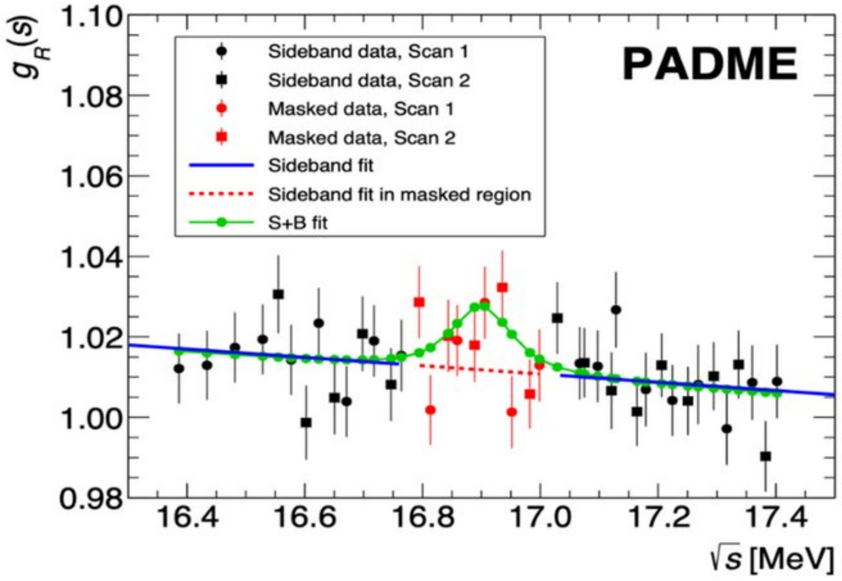

- At M_X = 16.90(2) MeV, g_{ve} = 5.6 x 10^{-4}, the global probability dip reaches 3.9 $_{-1.1}^{+1.5}$ %,
  - corresponding to (1.77 ± 0.15) one-sided (look-elsewhere calculated exactly from the toy pseudo-events)

- The observed limit is consistent with the expected within 1 sigma in most of the scan interval
  - Verification of the analysis robustness and uncertainty estimations
- Slight excess observed beyond the 2 σ local coverage

INCONCLUSIVE ON THE EXISTENCE OF X17

HOW TO IMPROVE?

NEW RUN IN 2025

- **RUN IV of PADME was with a largely modified setup**
  - A new large area charged particle detector with a novel readout plane design installed and operated for a first time - PADMME
  - Charged particle identification, tracking -> additional material in front of the ECal
  - The geometrical acceptance of the experiment was modified:
    - Moving downstream the diamond target
    - Removing passive material both inside the vacuum chamber and in front of the luminosity calorimeter
  - A new beam monitoring device installed substituting the Timepix3 detector - TMM
  - A new calibration and response monitoring system for the luminosity measurement detector
- **Measures for continuous monitoring of critical parameters**

More than an year of R&D, performance evaluation and ongoing data analysis (only the target movement took ~ 6 months)

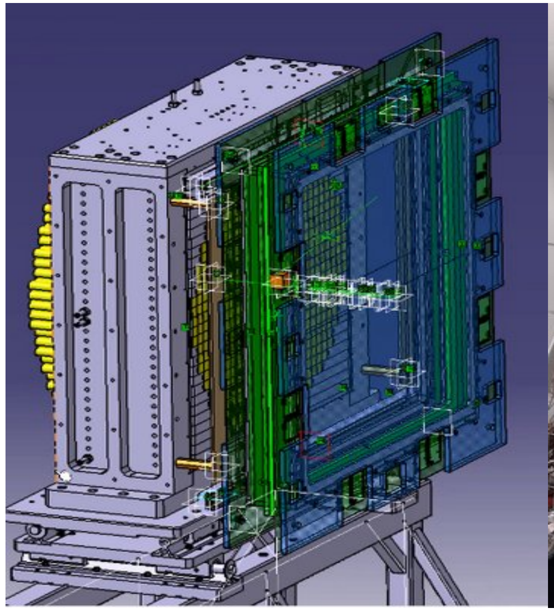

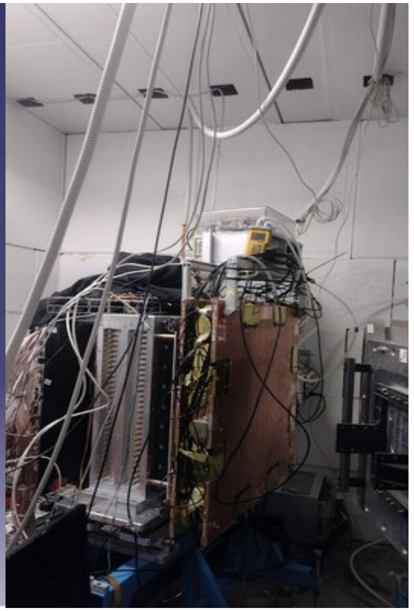

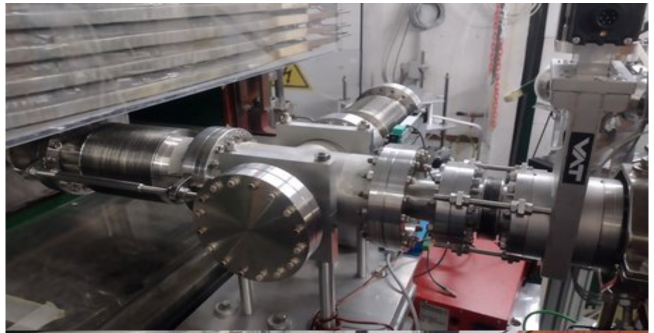

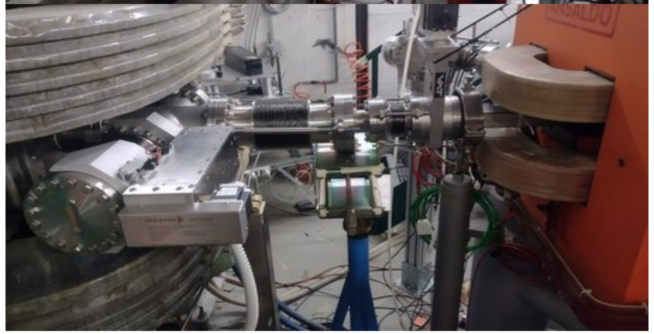

- Increase of acceptance
- Decrease the effect of the magnet ”shadow”

RUN IV acceptance increase

Run period	Target-Ecal distance	θ_{lab} @ 17 MeV	R_{range} @ 17 MeV	R_{max} from magnet
RUN III	3700 mm	48 – 73 mrad	177 – 270 mm	249 mm
RUN IV	3360 mm	43 – 80 mrad	146 – 270 mm	268 mm

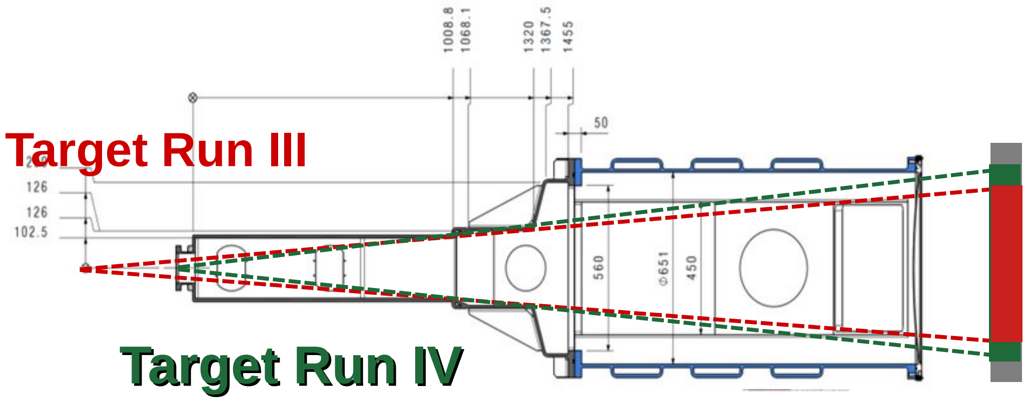

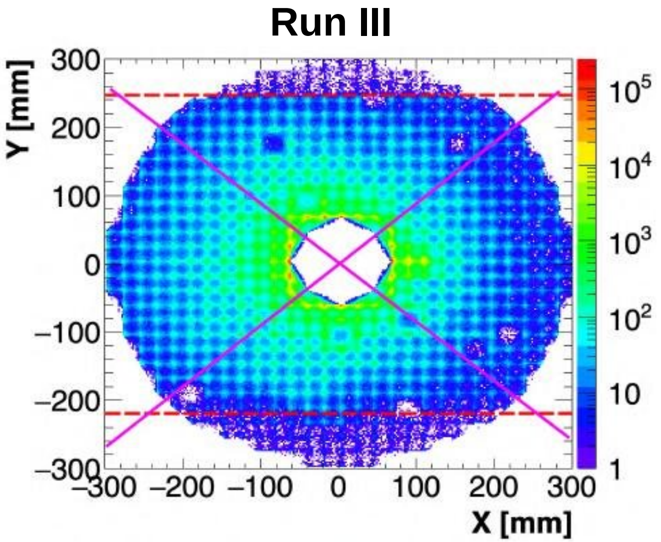

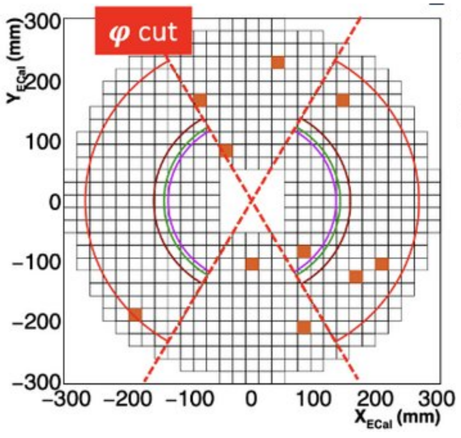

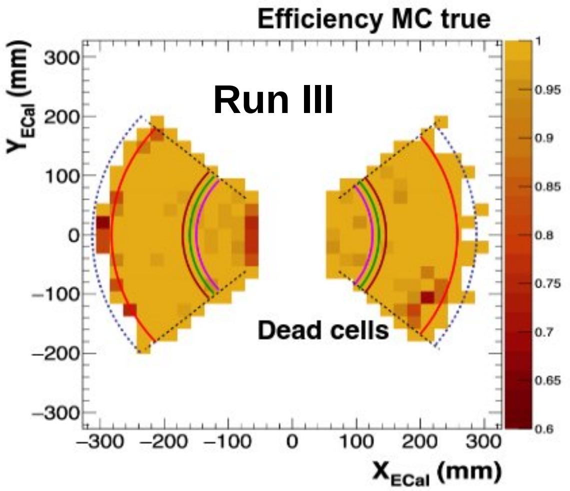

- φ-cut can be removed or adapted
  → uniformity in the acceptance
- Acceptance region widened
  → S/√B increases
- N_2 yield increases by a factor of ~ 2.5
  - Run III data: $\mathbf{N_2/N_{poT} \approx 3.7 \times 10^{-6}}$
    evaluated over ~0.8×10^{10} PoT
  - Run IV data: $\mathbf{N_2/N_{poT} \approx 9.9 \times 10^{-6}}$
    evaluated over ~10^{10} PoT

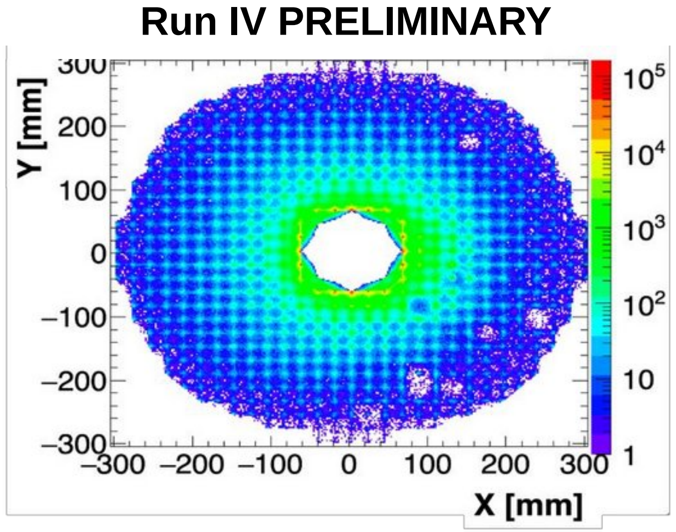

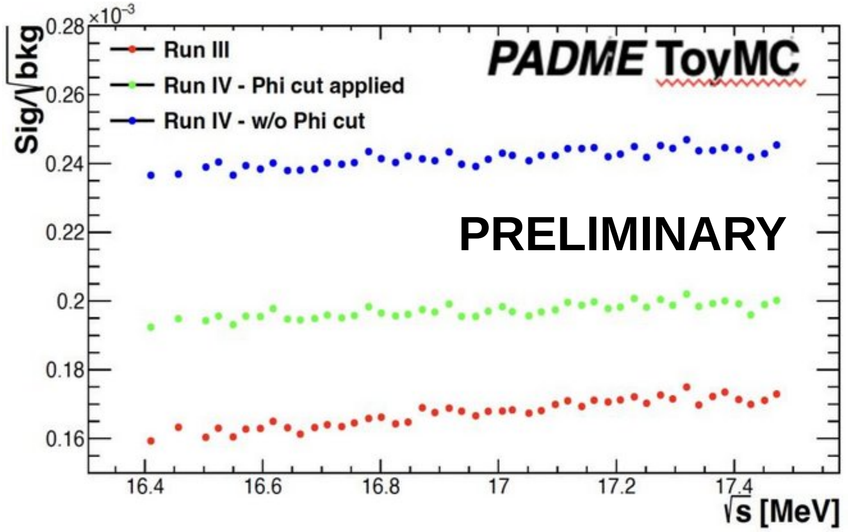

PADME Micromegas

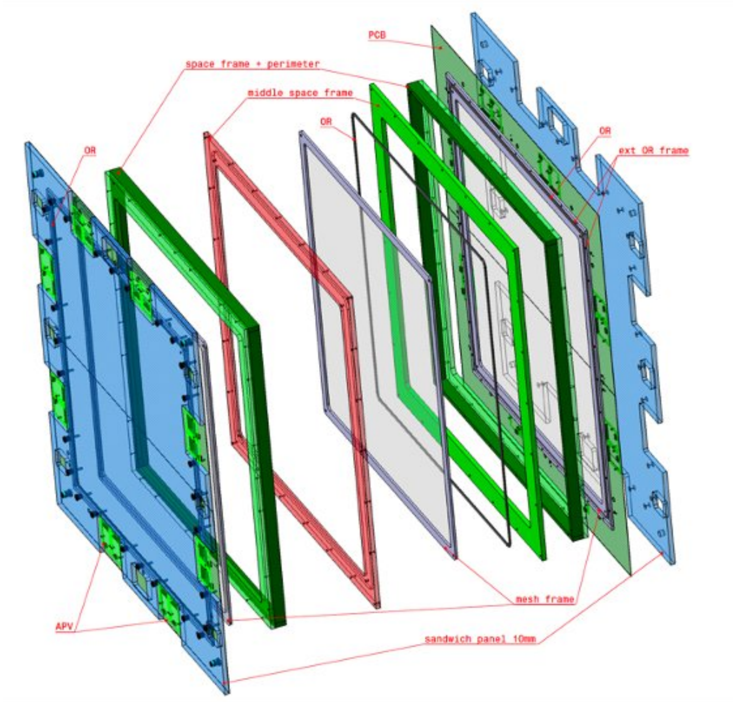

- A novel micromegas readout plane suggested
  - Rhomboidal pads for X and Y direction, decrease the mutual capacitance
- Variable HV depending on the distance from the beam center
  - Low HV in the center, measure the beam multiplicity
    - Additional control on the PoT
  - Higher HV in periphery to ensure close to 100 % efficiency

$HV_1 > HV_2 > HV_3$

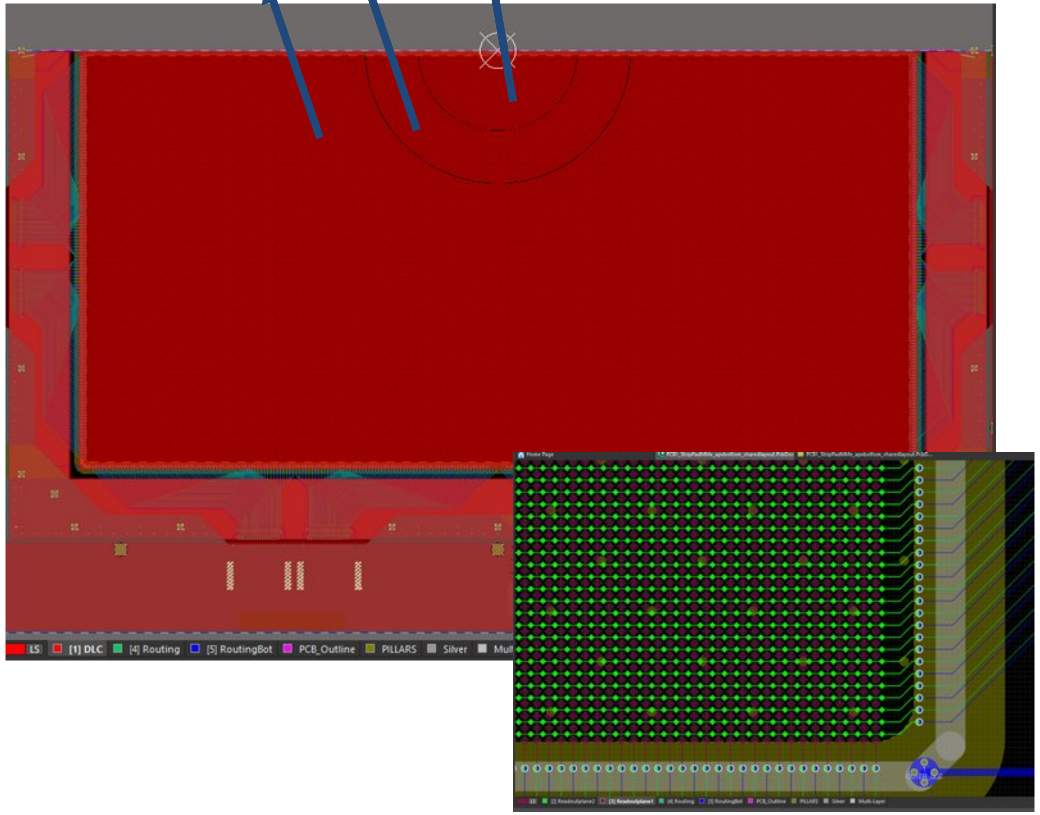

- Gas mixture: $Ar:CF_4:i\text{-}C_4H_{10} = 88:10:2$
- Readout - SRS system with APV ASIC hybrid
  - Timing and event matching
- Signal PCB layout inspired from smartphone capacitive touchscreen

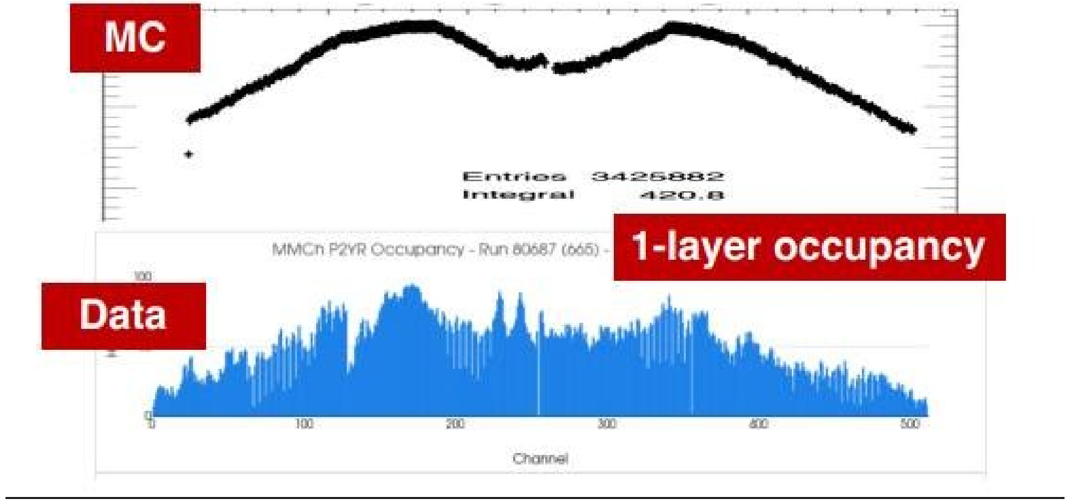

Track reconstructions

- Large combinatorial contribution in standard pattern recognition
  - ~3500/4096 fired strips ~85% occupancy
  - ~200 track candidates found w/o Interaction Point (IP) constraint
  - → IP-oriented pattern recognition algorithm
- Each charged particle measured in 2 planes – both X and Y coordinates
  - 4 tracks (2D) expected for charged particle → Level-0 tracks
  - High efficiency but a Level-0 track requirement has high combinatorial background component
  - Need at least 2/3 out of 4 coincidence
  - Two-plane coincidence → Level-1 tracks
  - Performances obtained with nominal Run IV beam intensity

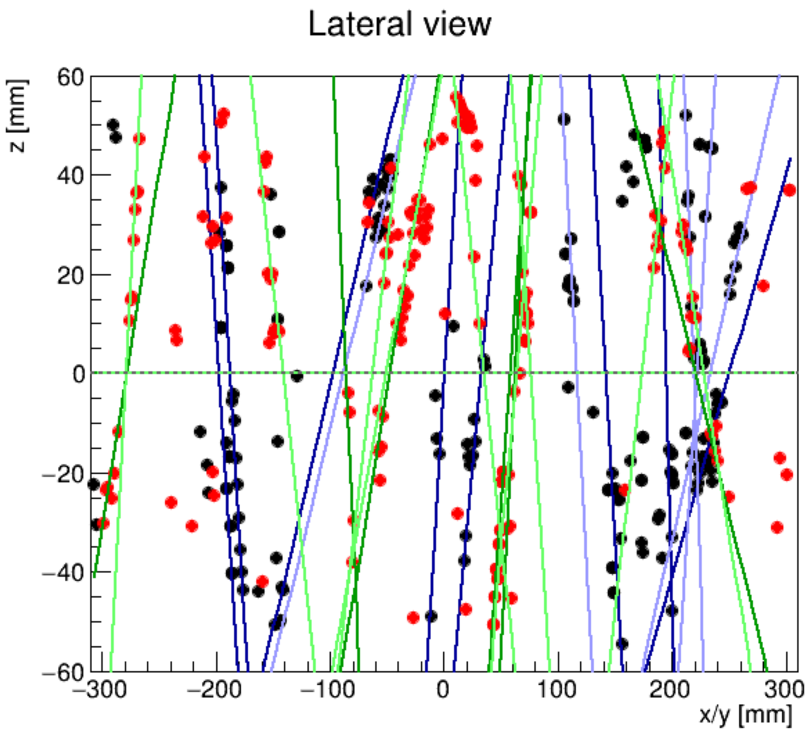

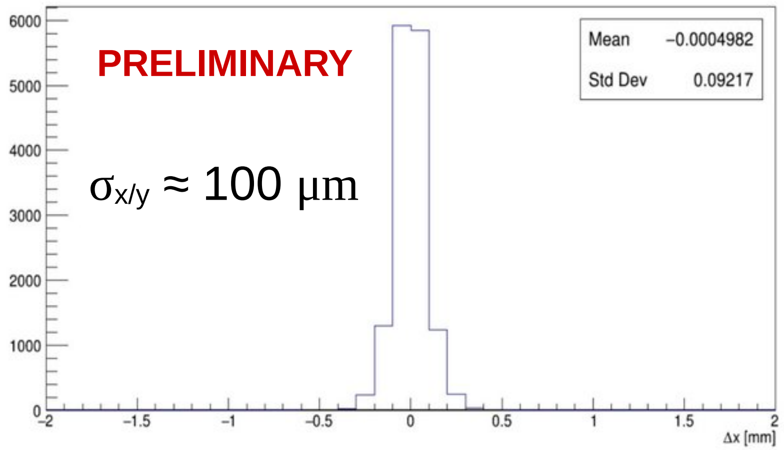

$\Delta x,y$ [mm]

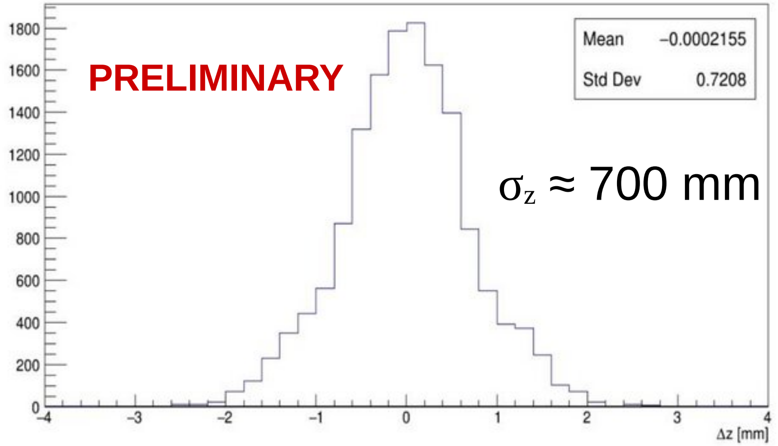

Δz [mm]

Track-to-Ecal-Cluster association

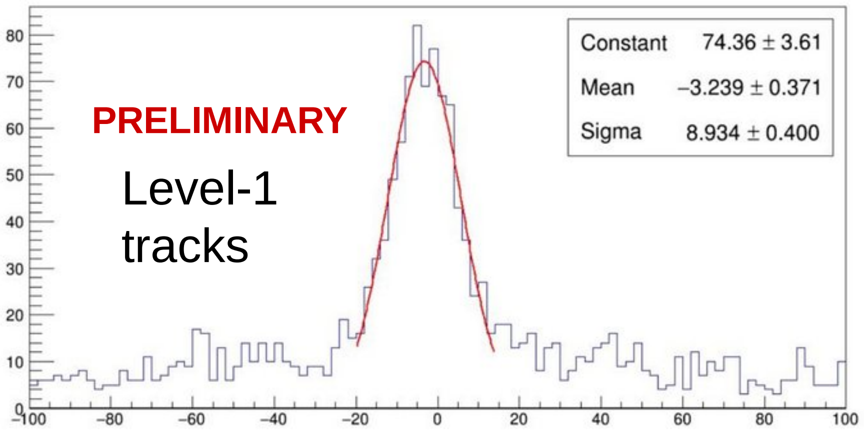

$\Delta x,y$ [mm]

Beam monitoring

- Knowledge of the beam parameters affects the precise determination of all quantities, used in the calculation of $g_R(s)$
- 4 measurement planes in RUN IV: Diamond Target, PadMME, ECal, TMM
    - position, angle, beam spread and beam divergence

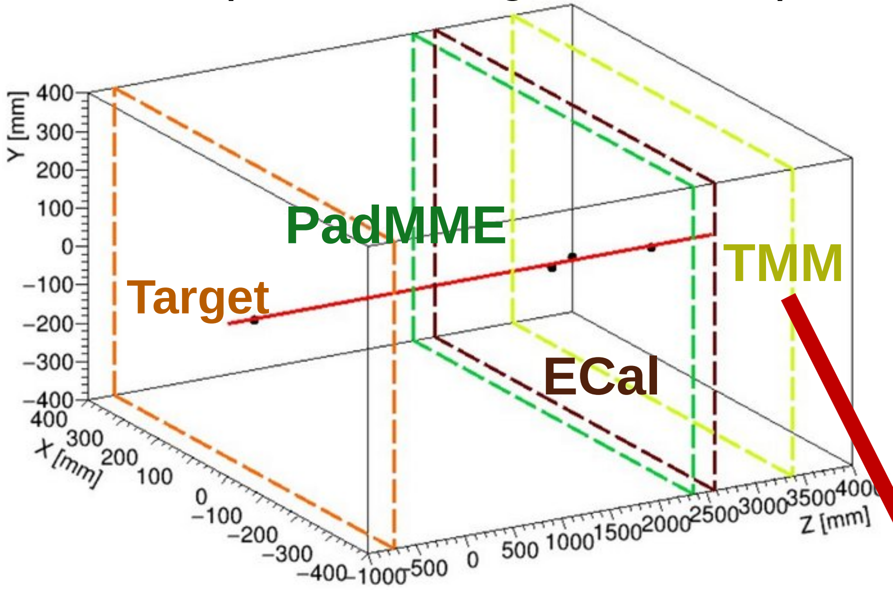

Beam spot at TMM

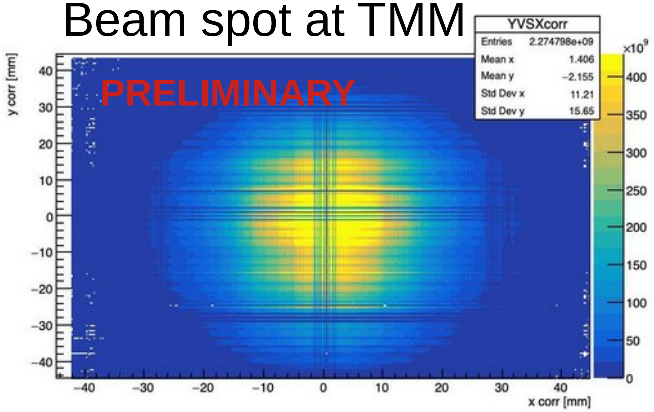

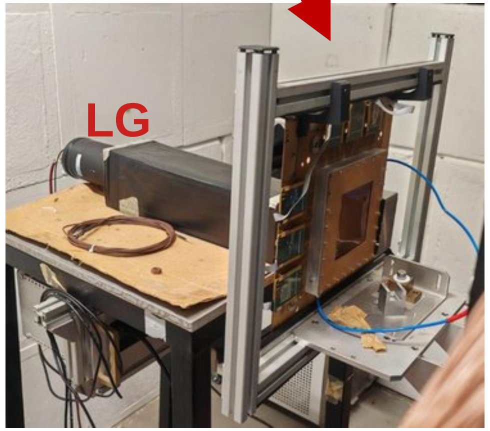

Target

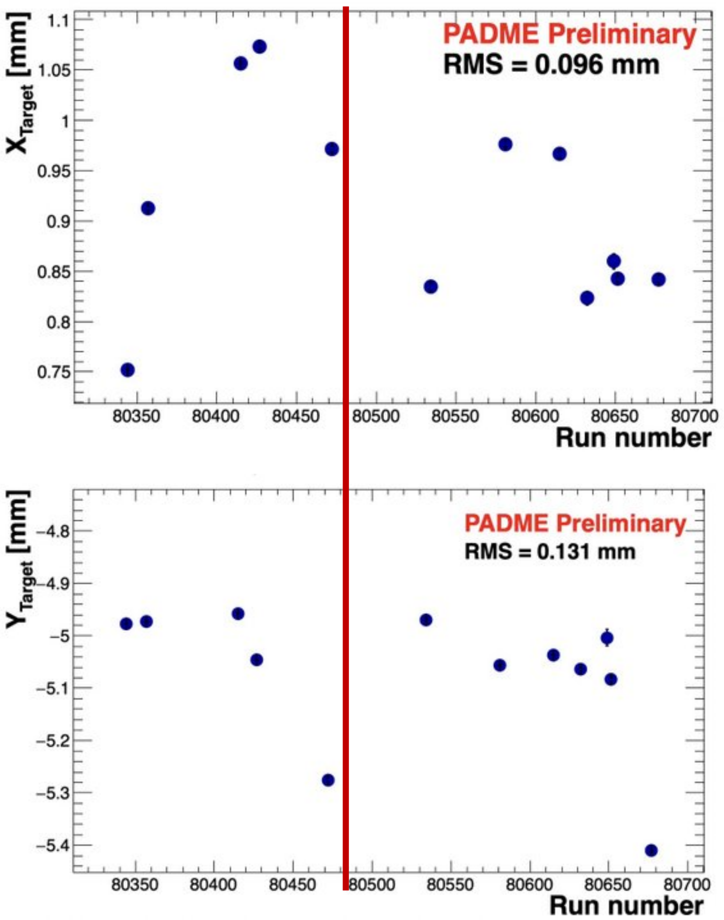

ECal

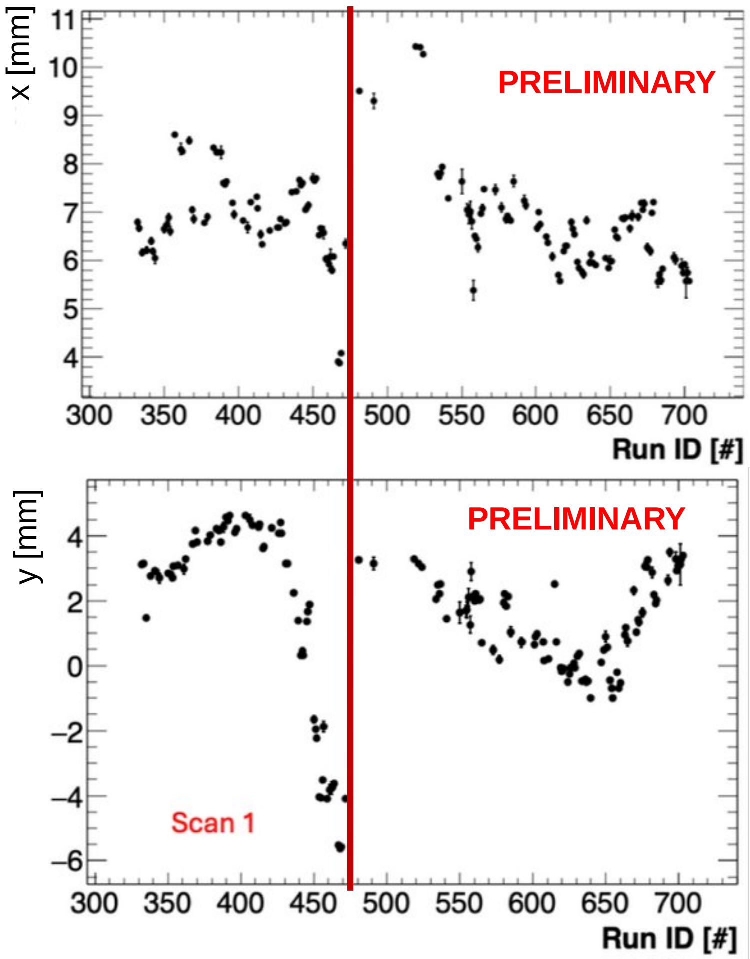

PADME RUN IV

- RUN IV execution
  - Started in April, 2025
  - Multiple issues (and fast decisions)
- Scan I: from Friday, 13.06 to 21.07
- Scan II: from 24.09 to 17.11
- O (2x10^{10} PoT) per point
- **Signal yield increase by ~2.5 with respect to RUN III**

AIMING FOR

Source	Uncertainty [%]
N_2	0.3
N_{PoT}	0.3
B	0.3
Total on g_R	0.5

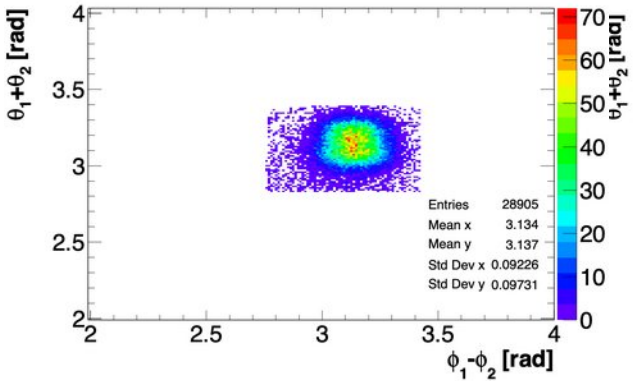

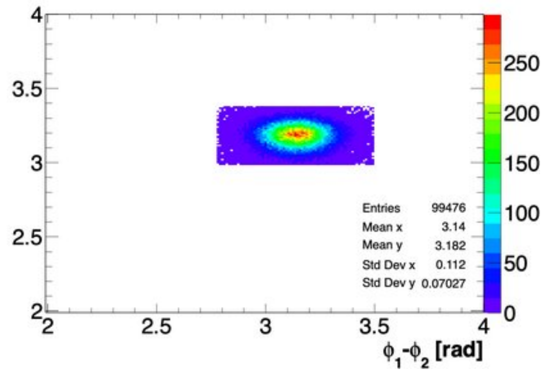

- 36 scan points, equally spaced by 0.75 MeV
- Improved sensitivity → aiming towards ~2 times reduction of the uncertainties

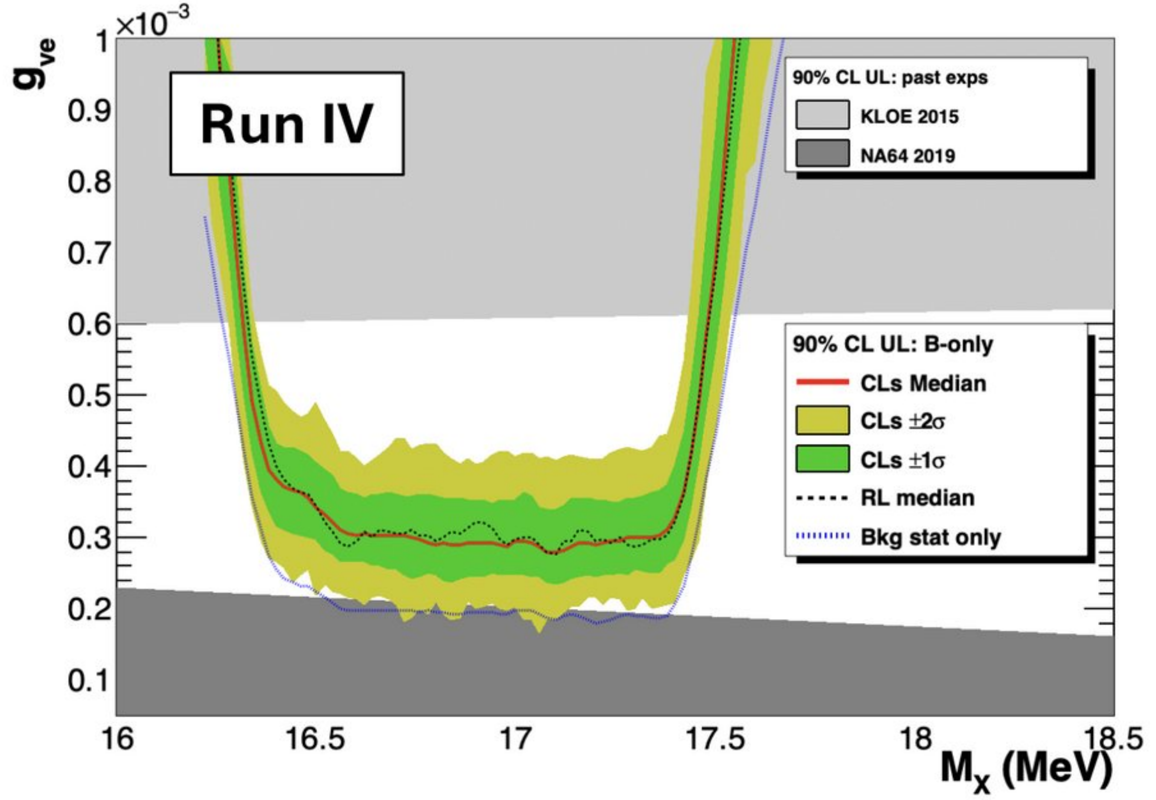

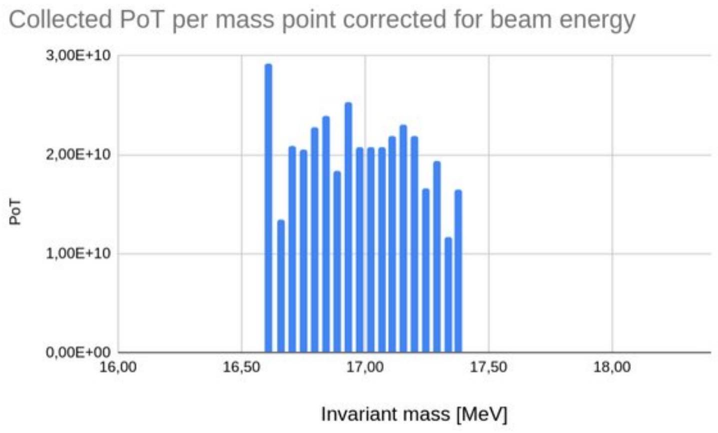

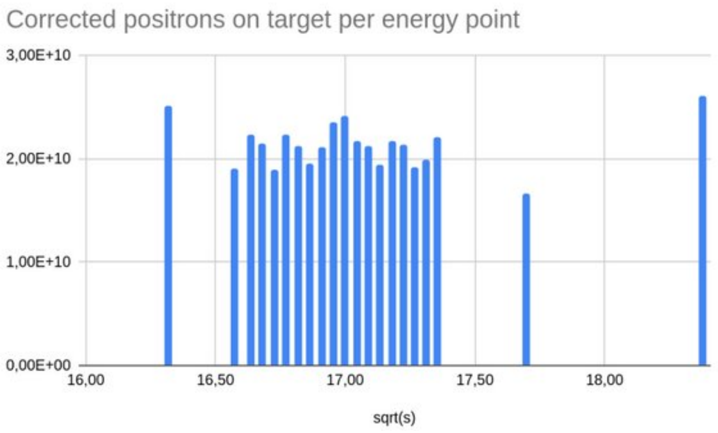

Conclusions

- RUN III X17 analysis completed
  - Overall uncertainty ~ 0.9 %
  - No indications for X17 above 2 sigma global p-value
  - An excess observed with a global p-value of 1.77 (0.15) sigma
- A major improvement to PADME setup for RUN IV
- Data taking finalized, 36 scan points with O(2e10) PoT each
- RUN IV data analysis ongoing

PADME will allow further probing of O(MeV) new particles

EXTRA MATERIAL

Relative signal/background acceptance

$$N_2(s) \,/\, (\, N_{POT}(s)\, B(s)\,) \quad = \quad g_R(s) \quad = \quad K(s)\,[\, 1 + S(s;\, M_X,\, g)\, \varepsilon_S(s) \,/\, B(s) \,]$$

Discriminate if $g_R(s)$ is consistent with
- **$K(s)$**, only Bkg with extra linear slope
- or
- **$K(s)\,[\, 1 + S(s;\, M_X,\, g)\, \varepsilon_S(s) \,/\, B(s) \,]$**

- Necessary to know both:
  - B(s): for the construction of $g_R(s)$
  - $\varepsilon_S(s)$ / B(s): for the discrimination between bkg only and bkg+signal hypothesis
- Expected background over signal efficiency determined from MC:
  - Run by run beam spot from COG
  - Cancellations of systematics in $\varepsilon_S(s)$ / B(s)
- Fit $\varepsilon/B(s^{1/2})$ with a straight line, include fit parameters as nuisances:
  - Errors: $\delta P0/P0 \sim 0.1\%$, $\delta P1/P1 = 3\%$, correlation = -2.5%
  - Separate fits for scan1 and 2, basically compatible
  - Behavior reproduced with toy MC

RUN-III definitions

- "**Run**": DAQ for ~8 hours, determine beam avg position/angle, ECal energy scale
- "**Period**": a point at a fixed beam energy, typically lasts 24 hours
- "**Scan**": a chronological set of periods typically decreasing in energy
- Scan 1 (12/10/2022 - 10/11/2022) and Scan 2 (25/11/2022 - 21/12/2022) spaced by ~ 1.5 MeV but interspersed in energy

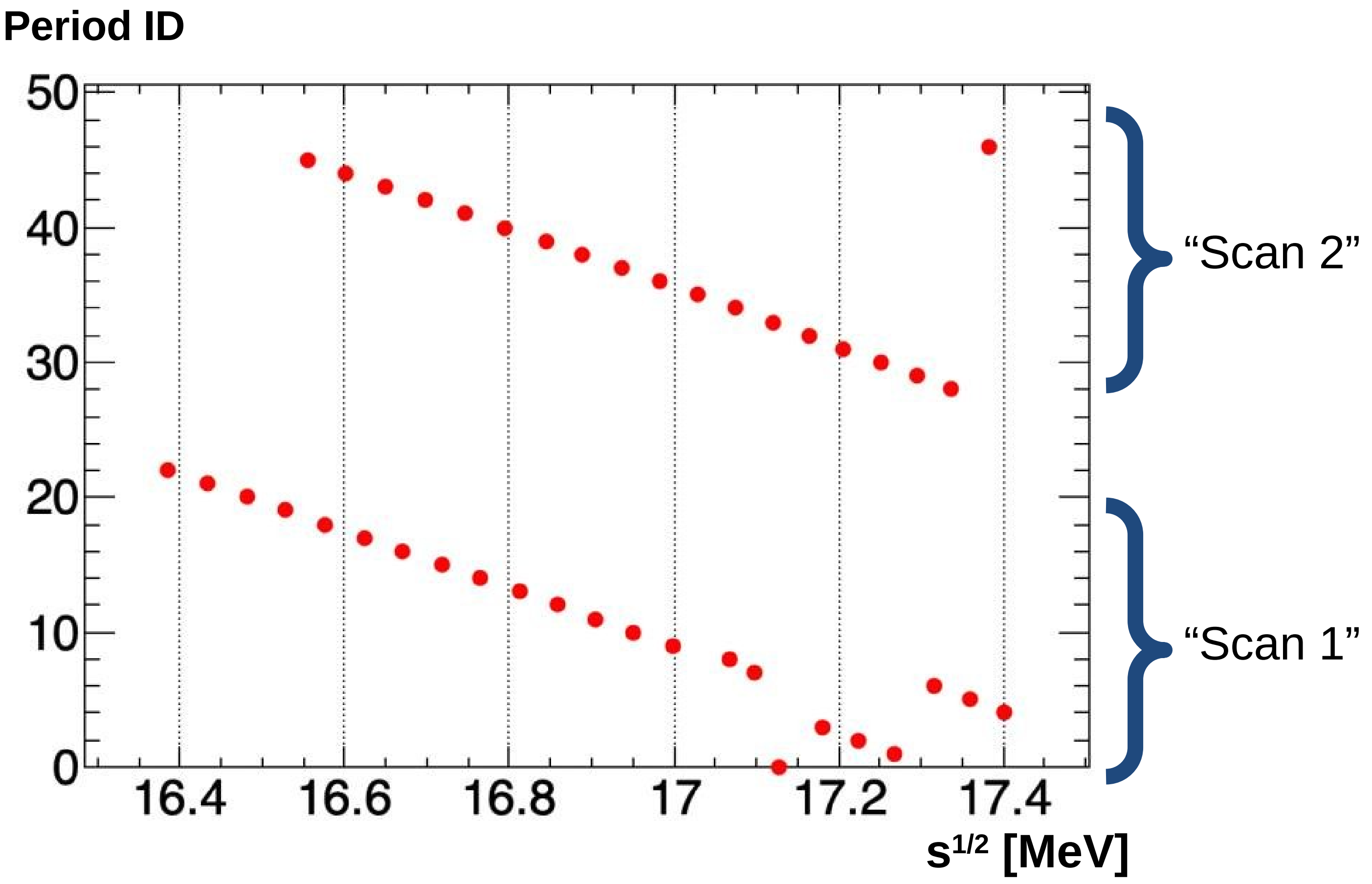

Collected ~ 6 x 10^{11} PoT; > 10^{10} PoT per period (i.e. per scan point)

Detailed GEANT4-based MC performed for **each period**

E pur si muove

Signal yield: theoretical input

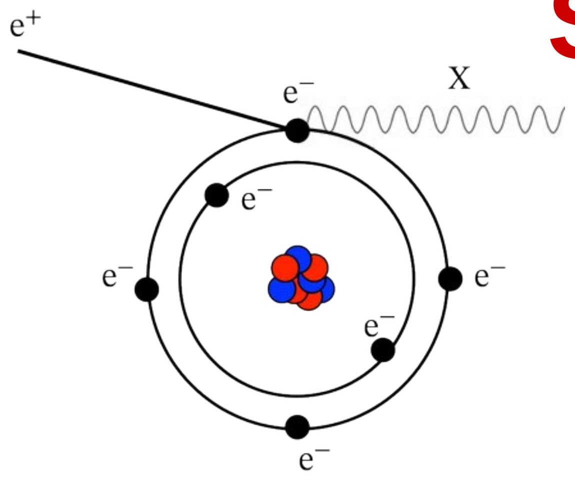

Motion of the atomic electrons in the diamond target from Compton profiles

$$d\sigma = \frac{d^3p_X}{(2\pi)^3}\int\frac{d^3k_A}{(2\pi)^3}\frac{(2\pi)^4}{8E_XE_AE_B|v_A-v_B|}\boxed{n\left(\vec{k}_A\right)}|\mathscr{M}|^2\delta^{(4)}(k_A+p_B-p_X)$$

- Line shape modification due to electron motion
  - Bound e^- momentum changes the e^+e^- invariant mass
- Peak height decreases, width increases, S/B decreases
- **$n(k_A)$** - electron momentum density function
  - Theory: calculate it using Hartree-Fock
  - Experiment: X-ray determination of electron momentum density

[Phys. Rev. 176 (1968) 900]

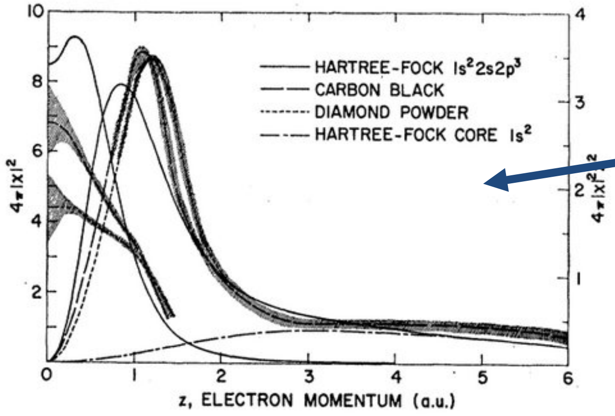

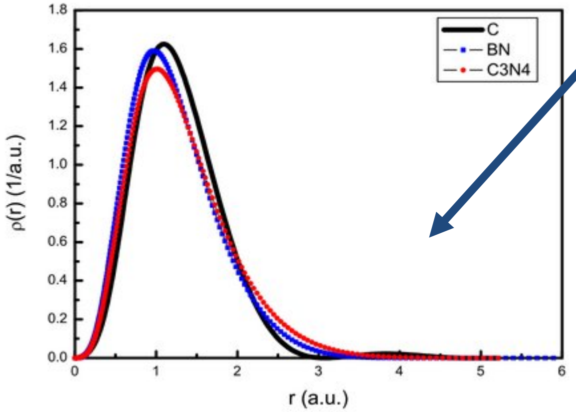

Physica B 521 (2017) 361–364

$S(E_{beam};\ M_X = 17\ \mathrm{MeV},\ g_v = 1)$

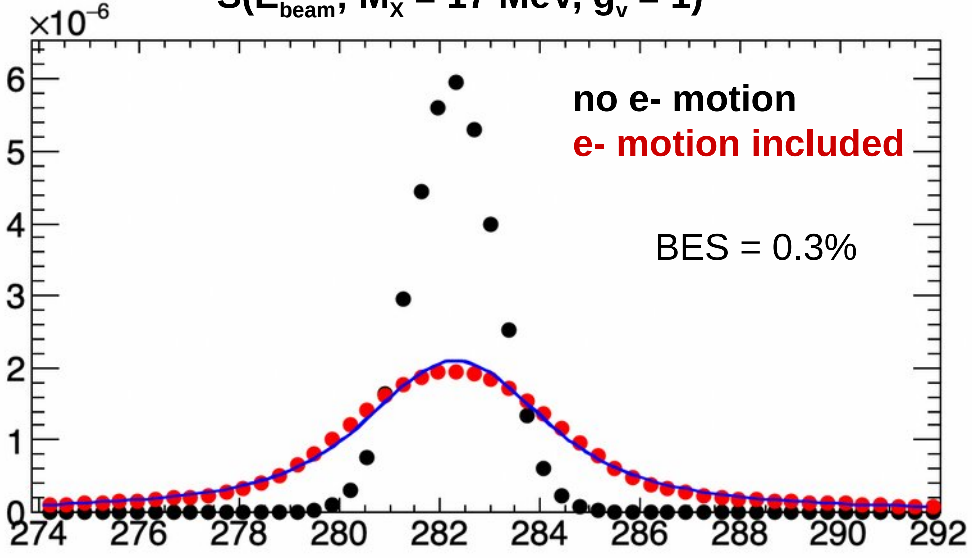

PRL 132 (2024) 261801

- **Parametrized signal yield as a function of E_{beam}**
  - **Convolution of Gaussian beam energy spread with Lorentzian**

    $\sigma_{res} = \sigma_{BES} \oplus \sigma_{Target}$
- **Lorentzian width of the peak: 1.72 (4) MeV**

Probing X17 in resonant production

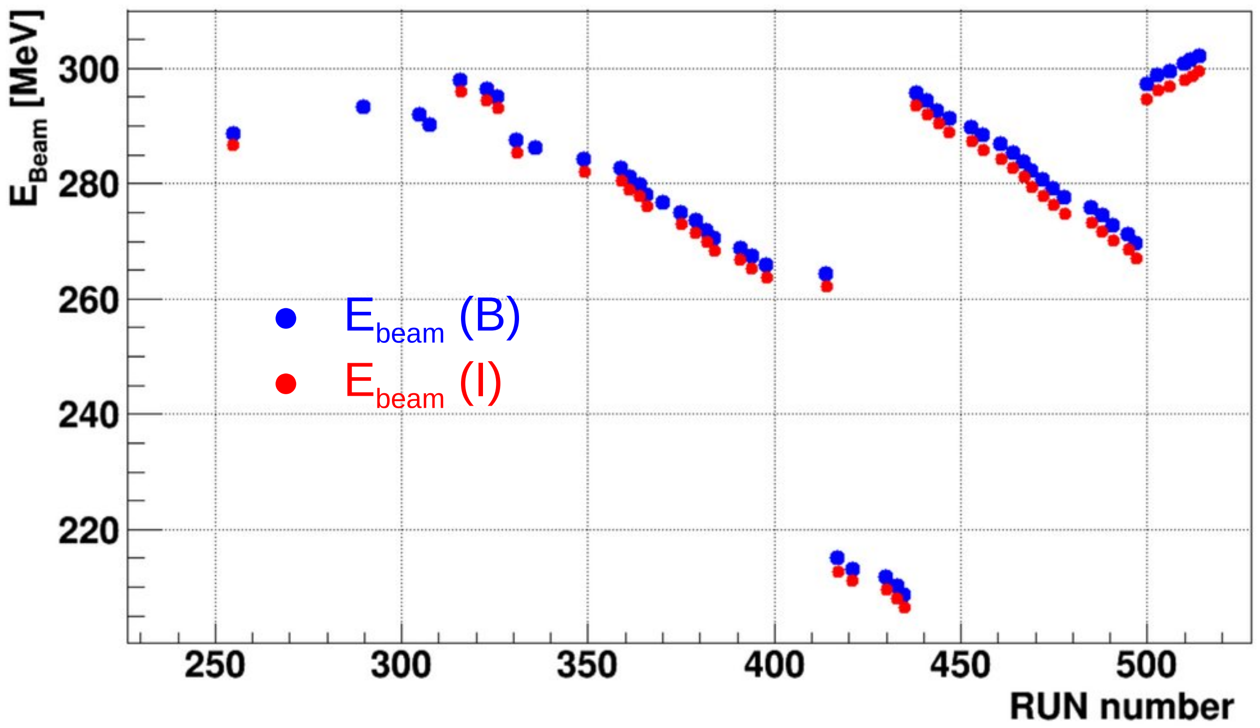

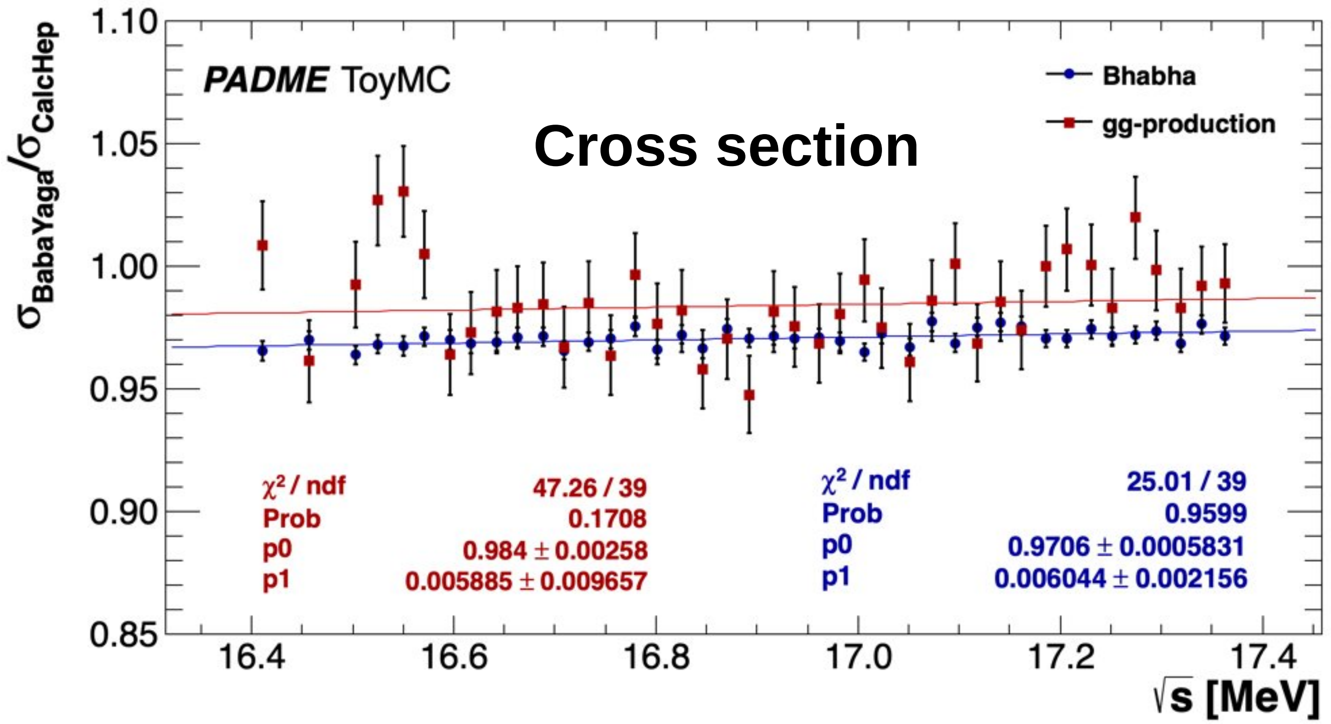

- Beam energy monitoring
  - Hall probe of DHSTB001 (dipole to BTFEH1)
    - P_{beam} [MeV] ~ 0.0551 x B [G]
  - Current of DHSTB001 [momentum selector] coils
    - Residual magnetization, variable during data taking
- Beam energy known to 1 % ⇒ systematics δM_{X17} ~ 30 keV
- Beam energy spread - defined by collimators and measured with no-target runs (no Coulomb scattering)
  - BES ~ 0.25 %

Comp.Phys.Comm. 184 (2013) 1729
Nucl. Phys. B 758 (2006) 227
Phys. Lett B 663 (2008) 209

- Radiative corrections with Babayaga
- Possible scale error of about ~2 %
- Possible slope on K(s) ~ 1.6 % MeV^{-1}

Data and upper limits comparison

Expected UL bands for:
- Background only
- Background + signal:

M_X = 16.9 MeV, g_{ve} = 5x10^{-4}

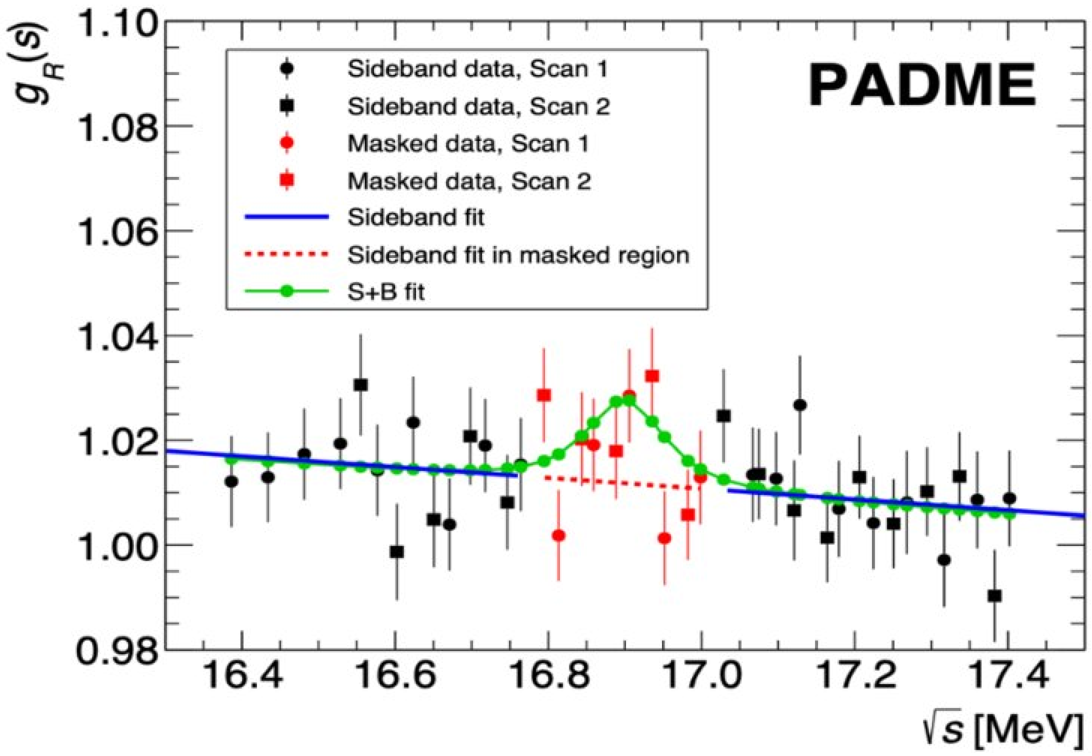

Masked by the automatic procedure

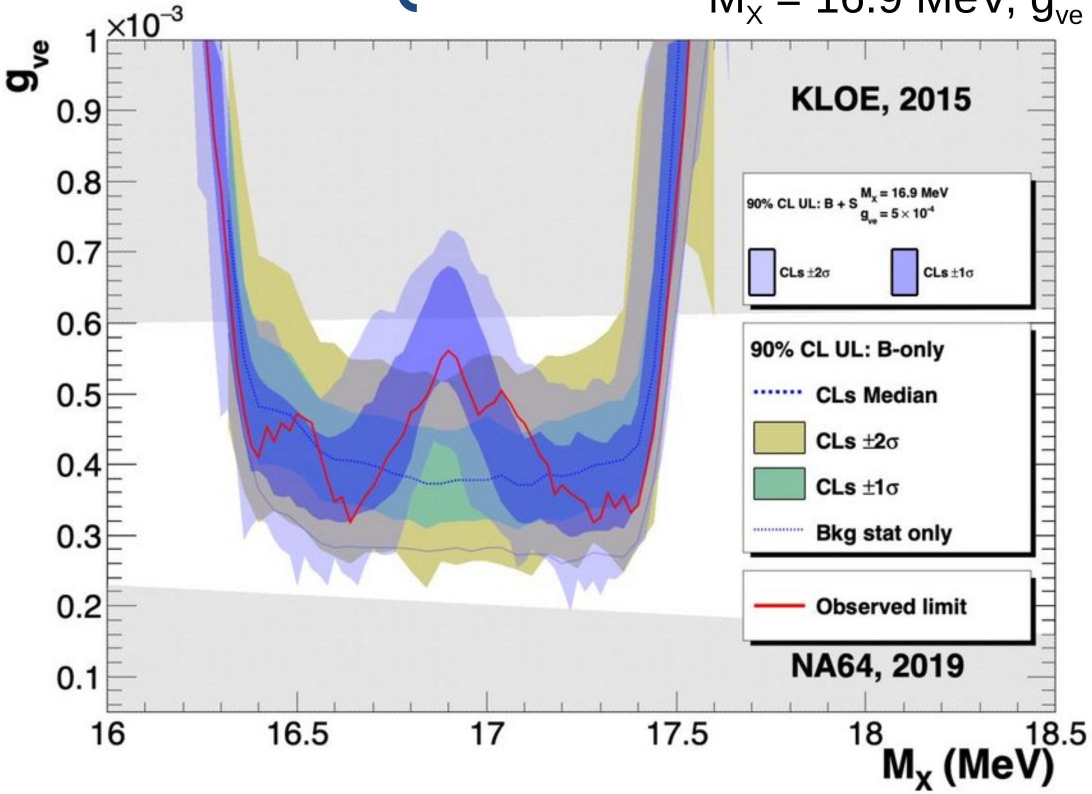

- ■ Masked point of scan 1
- ● Masked point of scan 2
- ■ Sideband point of scan 1
- ● Sideband point of scan 2

- **An extensive set of post box-opening tests performed**
  - test with K(s) = constant ⇒ **P(χ^2) = 74%** **same result confirmed**
  - test with power-constrained limit ⇒ **same result for the p-value**
  - test with different treatment of LG aging correction ⇒ **same result**
  - test with B(s) as straight lines (see B($s^{1/2}$) dependence) ⇒ **1.6 σ excess confirmed to be present**

Active target

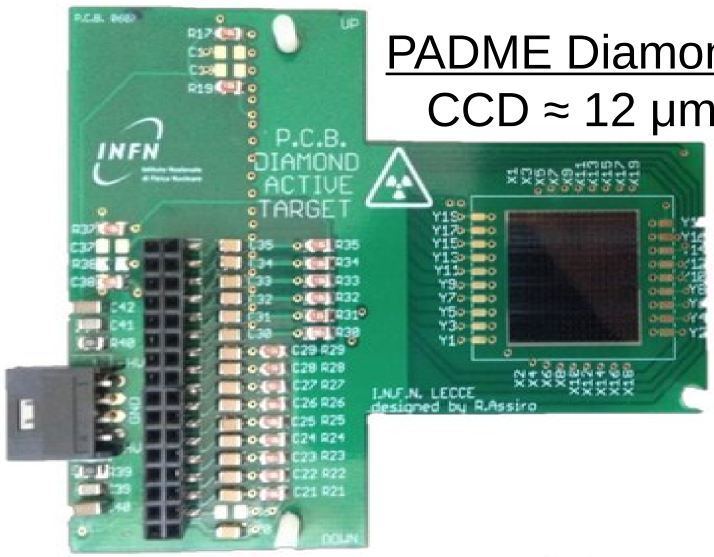

PADME Diamond

CCD ≈ 12 µm

JINST 12 (2017) 02, C02036

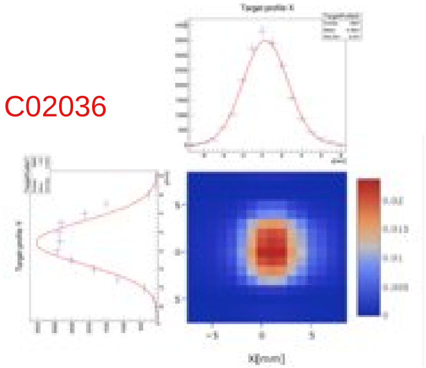

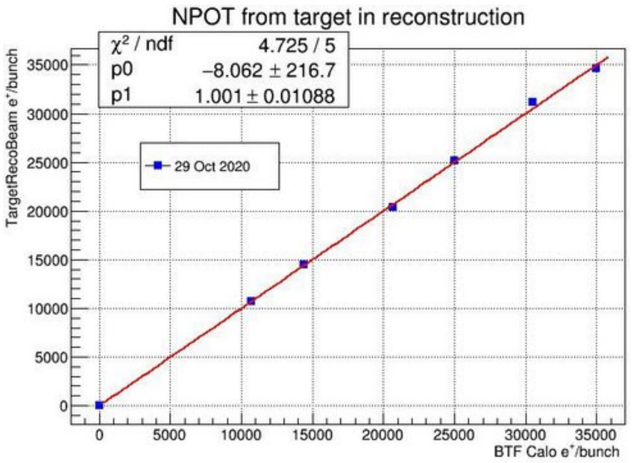

Charged particle detectors

Polycrystalline diamond

- 100 µm thickness:
- 16 × 1 mm strip and X-Y readout in a single detector
- Graphite electrodes using excimer laser

Extruded plastic scintillators with WLS fibers

- Three sets of detectors detect the charged particles from the PADME target (at E_{beam} = 550 MeV):
  - **PVeto**: positrons with 50 MeV < p_{e+} < 450 MeV
  - **HEPVeto**: positrons with 450 MeV < p_{e+} < 500 MeV
  - **EVeto**: electrons with 50 MeV < p_{e+} < 450 MeV
- 96 + 96 (90) + 16 (x2) scintillator-WLS-SiPM RO channels
- Segmentation provides momentum measurement down to ~ 5 MeV resolution

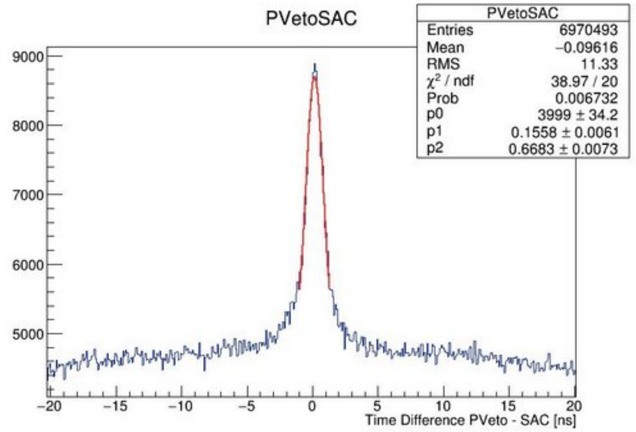

JINST 19 (2024) 01, C01051

- Online time resolution: ~ 2 ns
- Offline time resolution after fine T_0 calculation – better than 1 ns

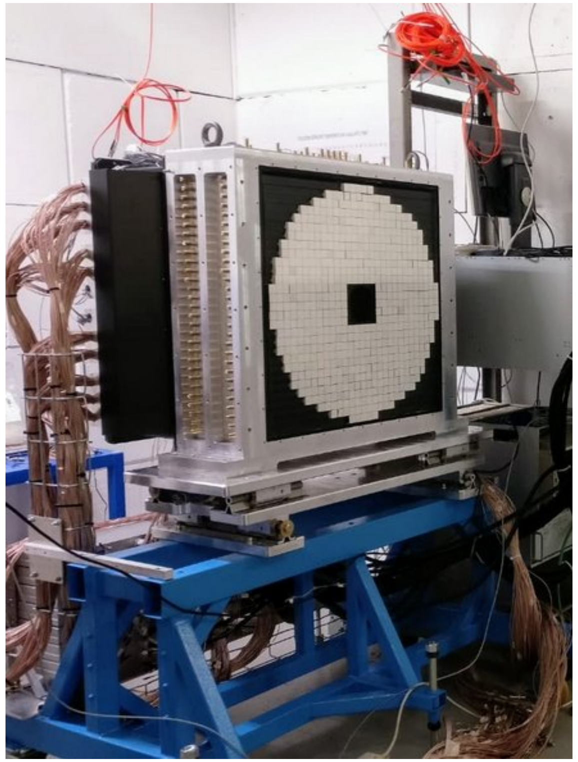

Calorimeters

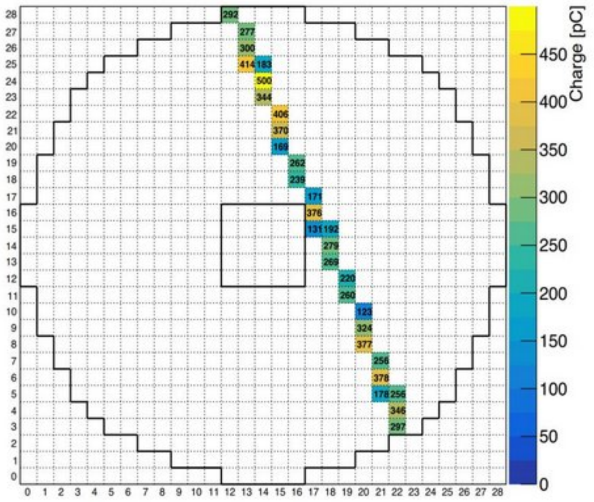

JINST **15** (2020) T10003

ECAL: The heart of PADME

- 616 **BGO** crystals, 2.1 x 2.1 x 23 cm^3
- BGO covered with diffuse reflective TiO_2 paint + additional optical isolation: 50–100 μm black Tedlar foils

Calibration at several stages:

- BGO+PMT equalization with ^{22}Na source before construction
- Cosmic rays calibration using the MPV of the spectrum
- Temperature monitoring

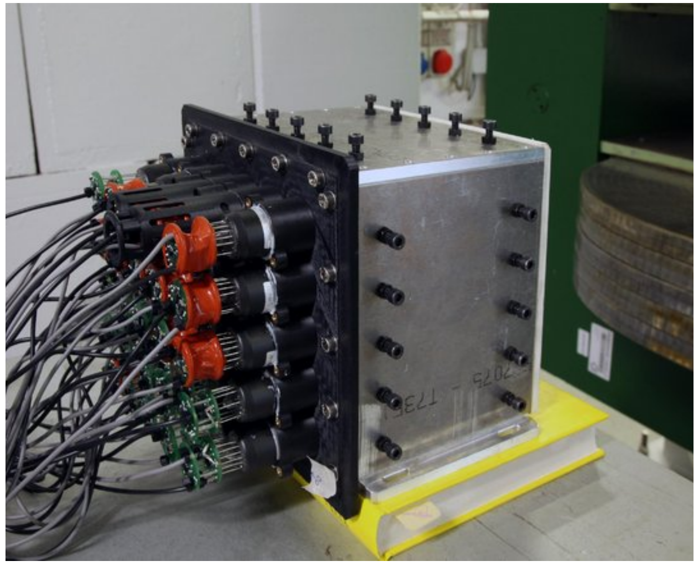

Nucl.Instrum.Meth.A 919 (2019) 89-97

Small Angle Calorimeter (SAC)

- 25 crystals - 5 x 5 matrix, Cherenkov PbF_2
- Dimensions of each crystal: 3 × 3 × 14 cm^3
- 50 cm behind ECal
- PMT readout: Hamamatsu R13478UV with custom dividers
- Angular acceptance: [0,19] mrad

Recorded bunch

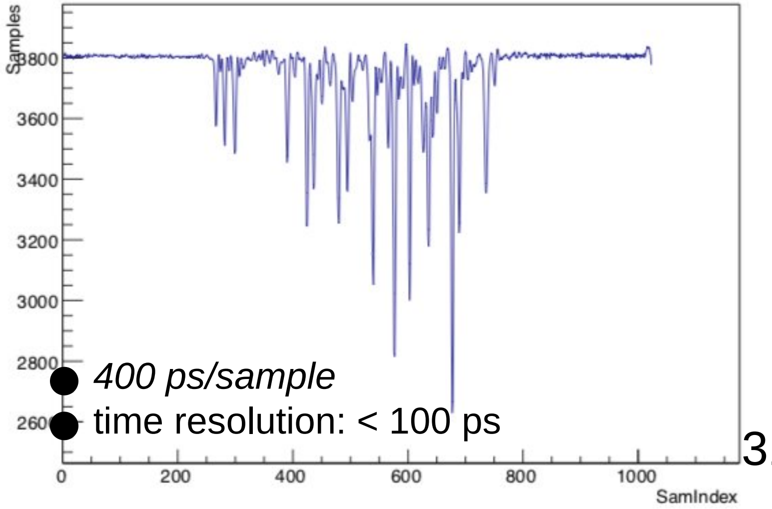

- *400 ps/sample*
- time resolution: < 100 ps

PADME RUN I and II

Run I and PADME commissioning

- Started in Autumn 2018 and ended Feb. 25th 2019
  - ~7 x 10^{12} PoT recorded with **secondary beam**
  - DAQ, Detector, beam, collaboration commissioning
  - Data quality and detector calibration
- PADME test beam data
  - July 2019, few days of valuable data
    - Certification of the **primary beam**
  - Detector performance/calibration checks
  - Primary beam with E_{beam} = 490 MeV

RUN II: primary beam

- July 2020
  - New environment/detector parameter monitoring and control system
  - Remote operation confirmation
- Autumn 2020:
  - A long data taking period with O(5x10^{12}) e^+ on target
  - E_{beam} = 430 MeV

20 000-30 000 e^+/pulse → pileup in the downstream detectors → new reconstruction techniques

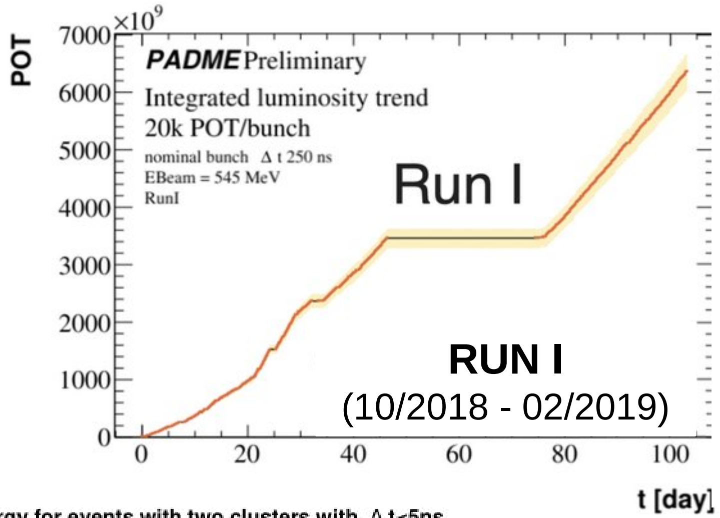

JINST 17 (2022) 08, P08032

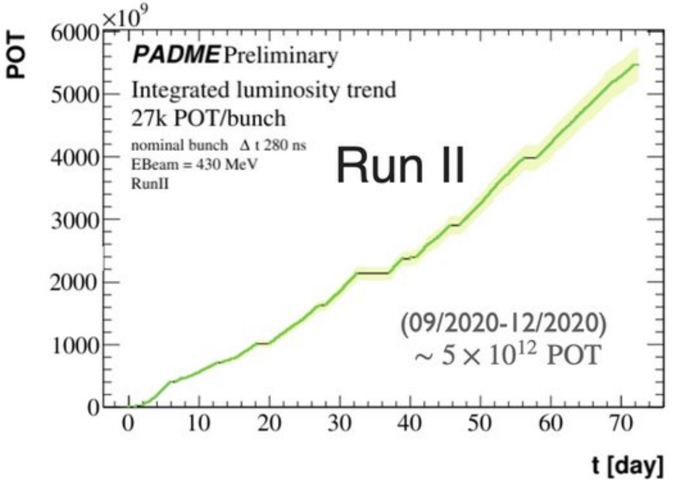

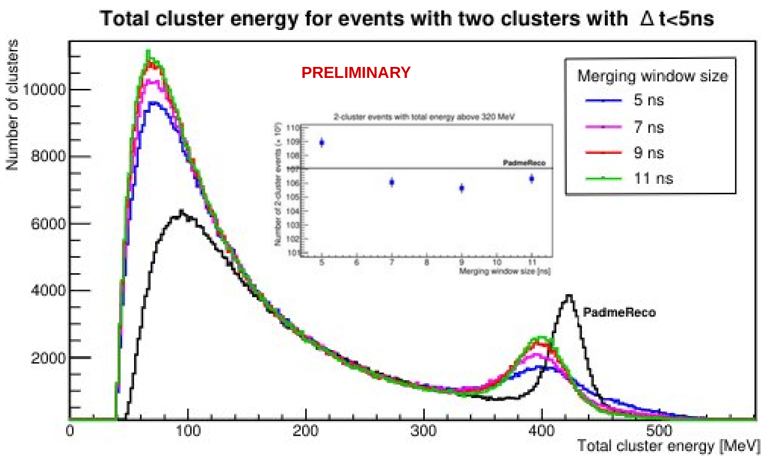

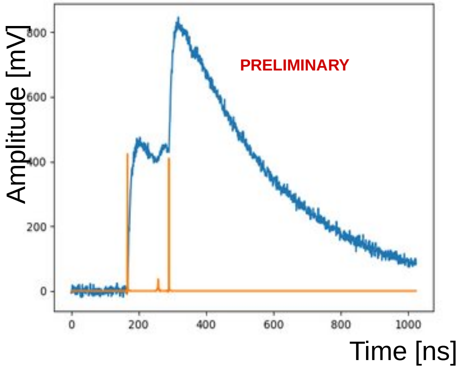

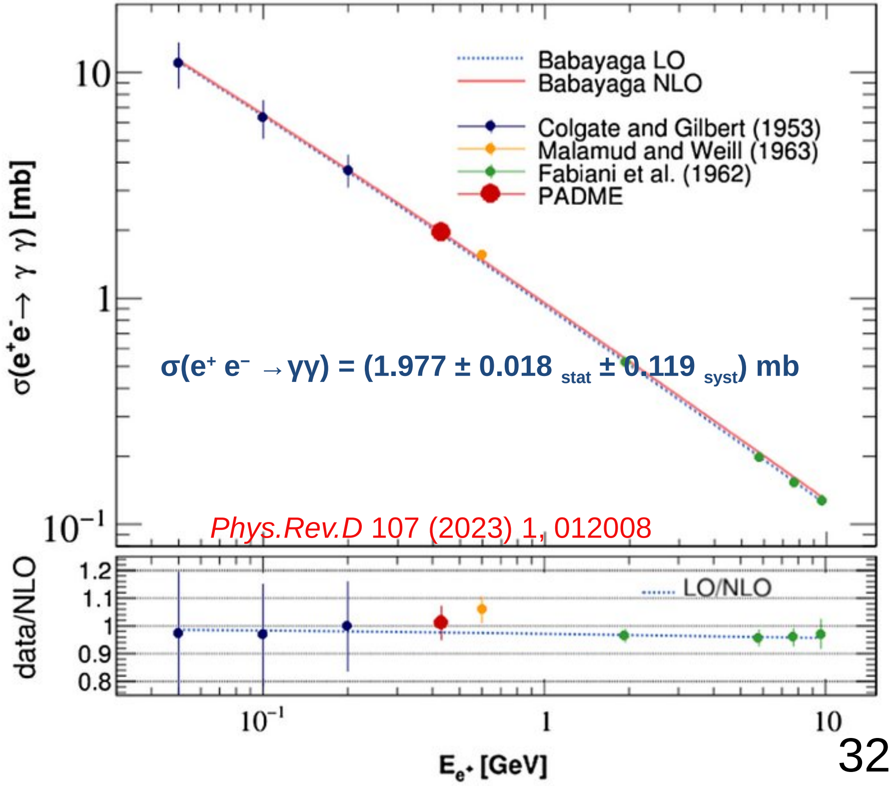

Positron flux measurement: beam influence

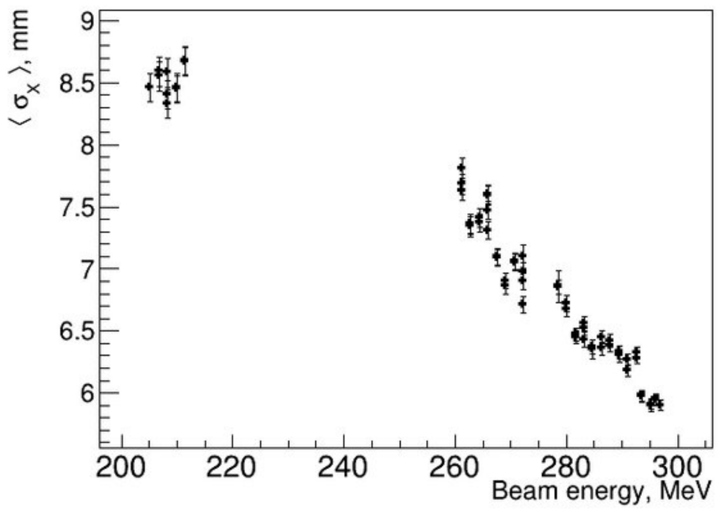

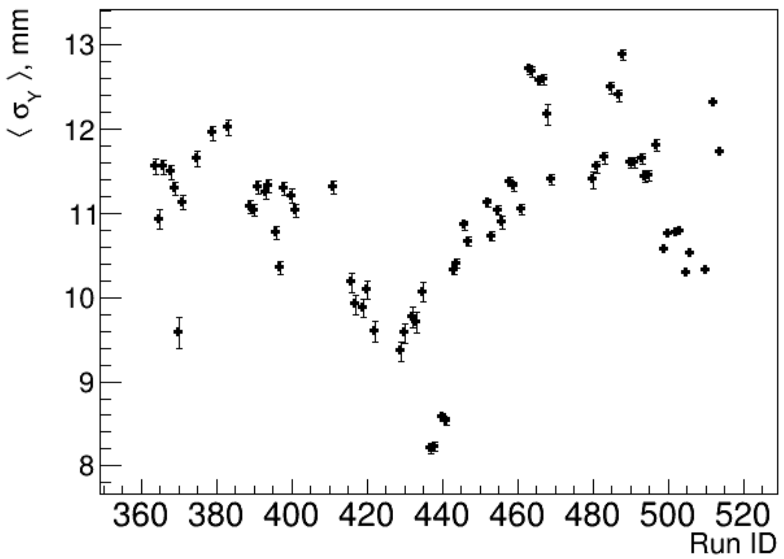

- The beam spread in Y direction varies within ~2 mm during the data taking
- The beam spread in X is energy dependent
  - However in X the containment is largely ensured

Particles impacting inside the TPix sensitive area

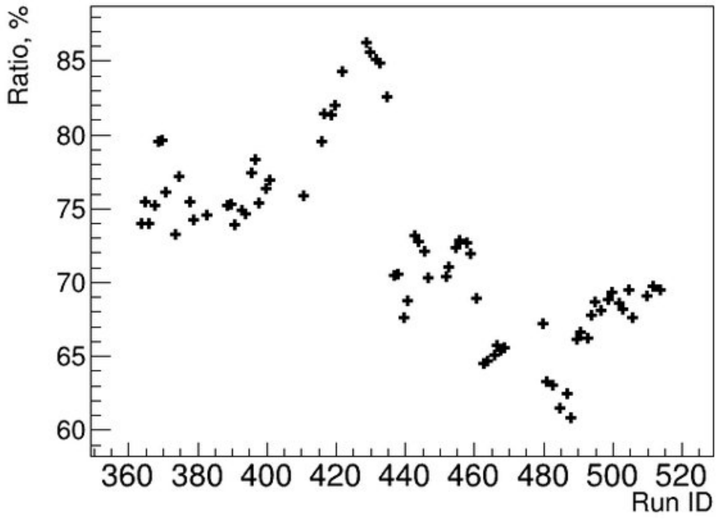

Correction due to the beam movement (convolution of TimePix & LeadGlass) results in systematics contribution < 1 %

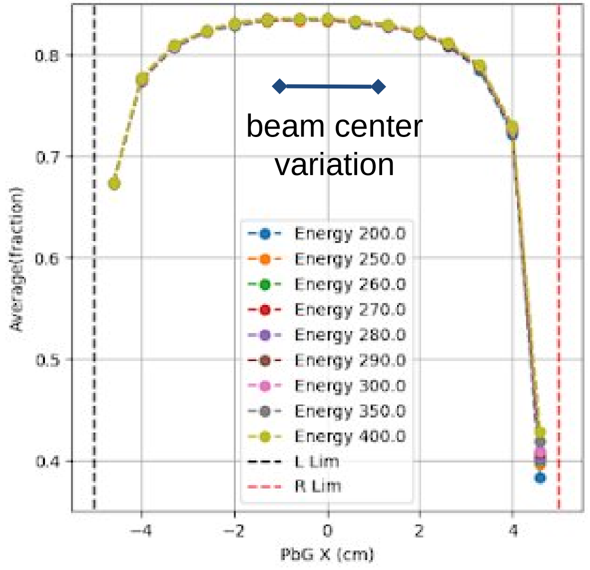

Average set at 0.875

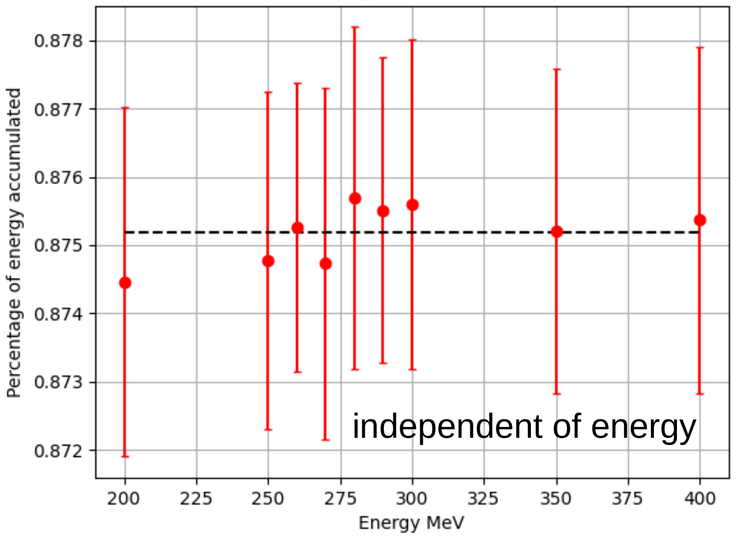

The energy containment correction uncertainty well below 1 %

N_2 events and background

Using side-bands (bremsstrahlung, ~4%)

N_2

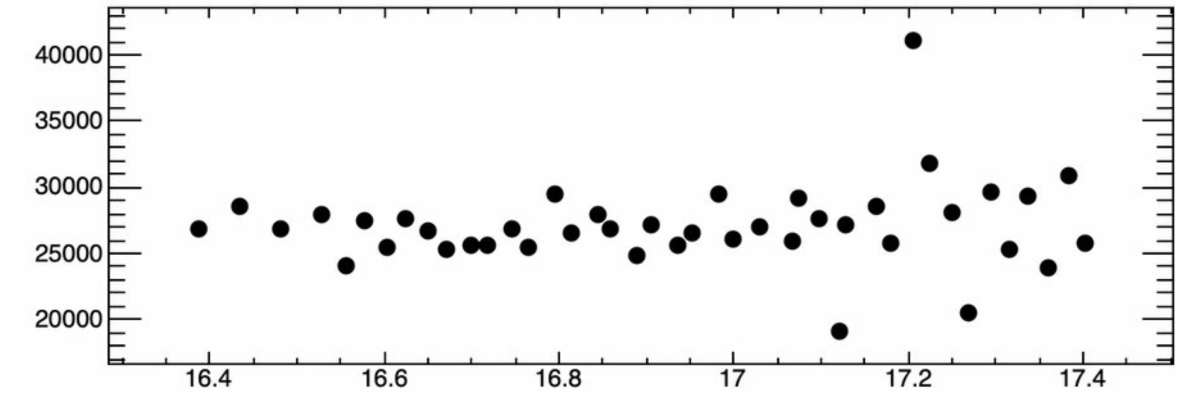

$\delta N_2/N_2$

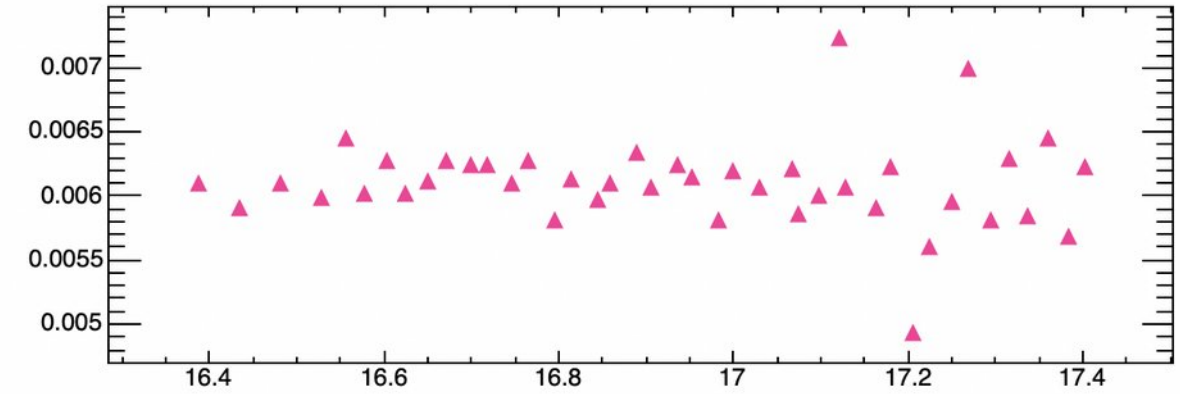

$s^{1/2}$ [MeV]

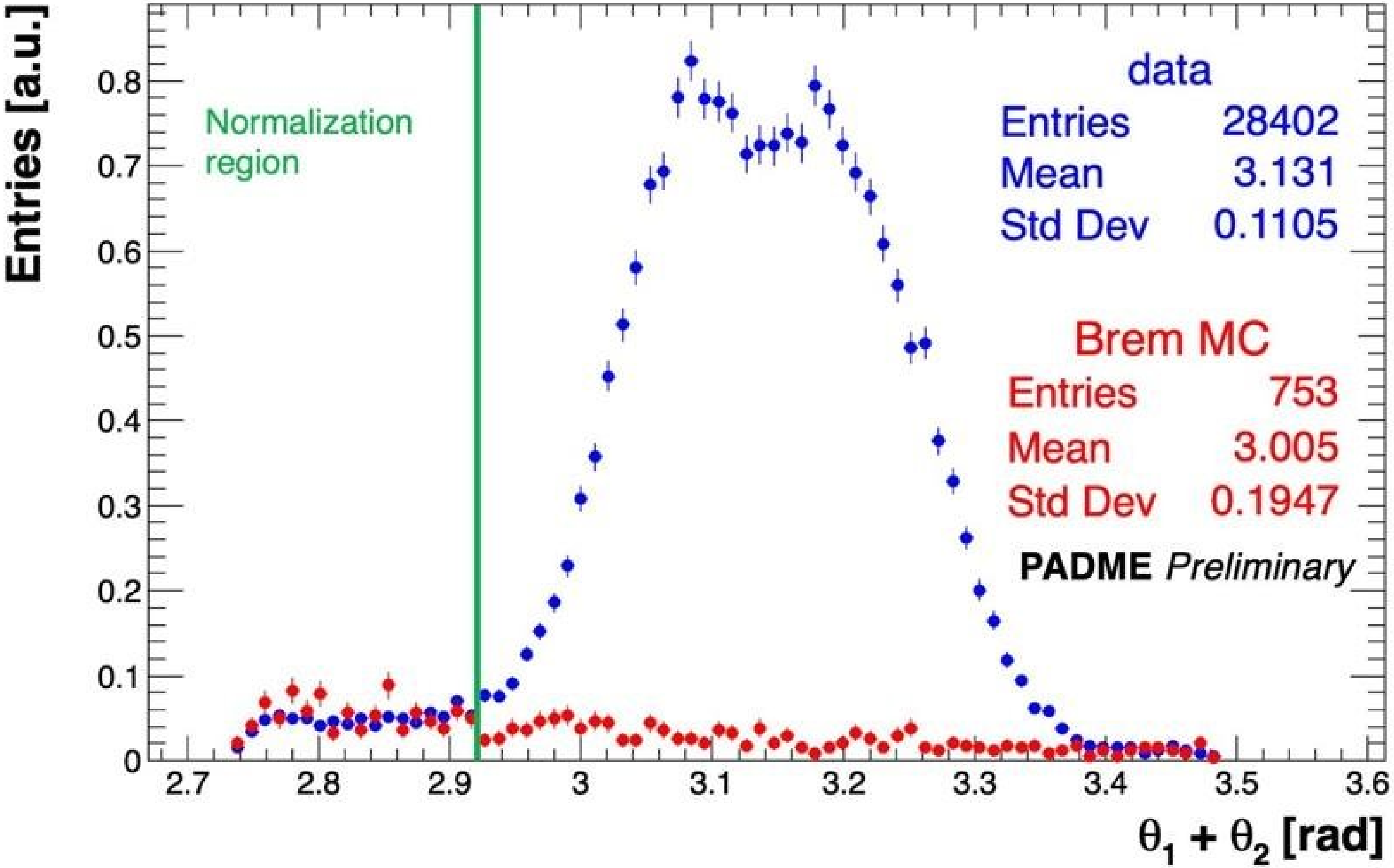

Double peak structure due to residual magnetic field
with ~ 13 Gauss